EFFECTS OF WEIGHTLESSNESS ON THE VESTIBULO-OCULAR REFLEX IN THE CREW OF SPACELAB 1

by

MARK JOHN KULBASKI

SUBMITTED TO THE DEPARTMENT OF
MECHANICAL ENGINEERING IN PARTIAL
FULFILLMENT OF THE
REQUIREMENTS FOR THE
DEGREE OF

BACHELOR OF SCIENCE

at the

MASSACHUSETTS INSTITUTE OF TECHNOLOGY

June 1986

Signature of Author [redacted]
Department of Mechanical Engineering
May 16, 1986

Certified by___
Charles M. Oman
Thesis Supervisor

Accepted by_____
Peter Griffith
Chairman, Department Committee

DISCLAIMER OF QUALITY

Due to the condition of the original material, there are unavoidable flaws in this reproduction. We have made every effort possible to provide you with the best copy available. If you are dissatisfied with this product and find it unusable, please contact Document Services as soon as possible.

Thank you.

Some pages in the original document contain pictures, graphics, or text that is illegible.

EFFECTS OF WEIGHTLESSNESS ON THE VESTIBULO-OCULAR REFLEX IN THE CREW OF SPACELAB 1

by

MARK JOHN KULBASKI

Submitted to the Department of Mechanical Engineering
on May 16, 1986 in partial fulfillment of the
requirements for the Degree of Bachelor of Science in
Mechanical Engineering

ABSTRACT

Slow phase angular eye velocity during a post rotational vestibulo-ocular reflex (PVOR) was studied pre and post flight in the crew of Spacelab 1, which orbited the earth for ten days in November, 1983. Six subjects were tested preflight. Four of those six flew on the mission and were tested postflight. Two separate vestibulo-ocular tests were performed.

First, subjects sat with the head upright in a chair that could rotate about the earth vertical axis. The chair was rotated at 120 degrees per second and then suddenly stopped. Eye movements were analyzed for 38 seconds after the stop. Subjects were tested in the clockwise and counterclockwise directions. Second, subjects were rotated at 120 degrees per second as before. However, they tilted the head down 5 seconds after the chair stopped and brought the head upright ten seconds after the chair stopped. Tests were carried out in both directions.

Slow phase eye velocity profiles of the PVOR head up tests from 1 to 20 seconds were fit to a first order model with time constant and gain. Likewise, head down velocity profiles between 5 and 10 seconds were fit to first order models. The mean preflight head up time constant +/- on standard deviation obtained by averaging mean population responses over five preflight days was 11.7 +/- 0.9 seconds. The head down time constant was 3.2 +/- 0.8 seconds. The gain was 0.59 +/- 0.1 seconds. The mean postflight head up time constant obtained by averaging mean population responses over the first two test days after landing was 9.3 +/- 0.3 seconds. The head down time constant was.3.4 +/- 1.5 seconds. The gain was 0.60 +/- 0.03 seconds.

A chi-squared test indicated that preflight vs postflight head up velocity decay profiles were significantly different between six and twenty seconds after the chair was stopped. Chi-squared tests indicated that both the pre and post flight head up and head down response profiles were significantly different between 5 and 10 seconds, respectively.

Thesis Supervisor: Dr. Charles M. Oman
Title: Senior Research Engineer of Aeronautics and Astronautics

ACKNOWL GMENTS

I wish to express my gratitude to my thesis advisor, Dr. Charles M. Oman, for his guidance, insight, and sustained encouragement during the course of this work. I also thank Sherry Modestino for invaluable support on the MVL computer system, Dr. Alan Natapoff for helpful criticisms on the statistical analysis, and Brian Rague for helping to produce the plots. Eve Riskin's careful documentation of the raw data made this investigation possible.

This thesis is dedicated to my father and mother.

Table of Contents

List of Figures

List of Tables

Chapter 1

Introduction

The purpose of this investigation was to study how adaptation to weightlessness affects the vestibulo-ocular system. The dynamics of post rotational slow phase eye velocity were examined preflight and postflight in the crew of Spacelab 1, which orbited the earth for ten days in November, 1983. Subjects were tested both with the head upright and with the head tilted forward five seconds after a step angular velocity from 120 degrees per second to 0 degrees per second about the vertical axis was applied to the head.

Benson and Bodin (1966) have shown that the apparent time constant of post rotational slow phase velocity is sensitive to the body's orientation to the gravity vector. In particular, they reported that the apparent time constant was less when the head and body were pitched forward or back than when the head and body remained upright. This suggests that the brain weighs information from both the otoliths or other gravireceptors with information from the semicircular canals to estimate angular head velocity.

The vestibulo-ocular system may adapt to weightlessness by reweighting or unweighting information from the gravireceptors. The brain may, in general reinterpret all sensory cues about body dynamics in weightlessness. Although control system engineers and physiologists have modeled how the inner ear can control eye movements, and anatomists have mapped basic neural pathways to support these models (Wilson and Jones, 1979), the vestibulo-ocular system is still not fully understood.

This study specifically documents preflight and postflight head up

and head down post rotational slow phase eye velocity to learn more about the structure and function of the vestibulo-ocular system by examining how it adapts to weightlessness.

Work required to complete this thesis involved processing experimental data which was recorded around the space flight, fitting the data to models, and analyzing the results.

A secondary result of this project was to test the performance of new digital filtering software which strips slow phase eye velocity from a signal of eye position. The algorithm was developed by Mohammed-Ali Massoumnia for a Master's Degree in Aeronautics and Astronautics at M.I.T. in 1983. In the past, oculomotor research routinely required processing large amounts of data by hand because no computer system was as accurate as a trained human to analyze a complicated electooculography (EOG) signal. This project would not have proceeded as quickly or as accurately without the new software.

Chapter 2

Background

2.1 Physiology and physics of the vestibulo-ocular system

Organs in the inner ear which detect motion are part of the "vestibular system." Muscles and their controllers which move the eyes are part of the "oculomotor system." The vestibulo-ocular reflex (VOR) refers to the phenomenon in which organs of the inner ear drive eye movement. If the angular velocity of the eyes were equal in magnitude and opposite in sign to the angular velocity of the head, there would be no retinal vision blur when the head moved. For the image of a target to remain stationary on the retina, the eyes must move as far and as quickly as does the head, though they must move in the opposite direction. Thus, to reduce vision blur during head rotation, the brain must measure the dynamics of head movement and then calculate appropriate compensatory eye movements.

Although the vestibular system does not directly measure head angular velocity or position, the semicircular canals serve as pseudo integrating angular accelerometers. There are three orthogonal semicircular canals on either side of the head. Each is filled with a fluid called endolymph, with properties similar to water. Angular acceleration of the head produces motion of the endolymph with respect to the canal walls, due to the inertia of the fluid. Displacement of the endolymph deforms a gelatinous structure called the cupula, which stimulates hair cells beneath it synapsing with afferent nerves. For brief head movements, distortion of the cupula produces negligible pressure forces on the ring of endolymph, compared to large viscous drag

from shear on the canal walls. Velocity of endolymph flow is proportional to acceleration of the head and cupula position is proportional to head velocity (Oman 1985).

Steinhausen (1931) and Van Egmond, et al (1949) have modeled the cupula-endolymph relation as a simple second order system with characteristic equation:

$$\ddot{\xi} + \frac{\pi}{\theta}\dot{\xi} + \frac{\Delta}{\theta}\xi = -\ddot{\beta} \qquad (1)$$

where θ is the moment of inertia of the endolymph ring about the center of the torus, π is the viscous drag coefficient of the endolymph on the canal wall, Δ is the stiffness of the cupula, ξ is the deformation of the cupula, and β is the angular position of the head. In the Laplace frequency domain, the transfer function of the system is:

$$\frac{\xi(s)}{\ddot{\beta}(s)} = \frac{-1}{s^2 + \frac{\pi}{\theta}s + \frac{\Delta}{\theta}} \qquad (2)$$

This can be approximately factored as

$$\frac{\xi(s)}{\ddot{\beta}(s)} = \frac{-1}{(s+\frac{\pi}{\theta})(s+\frac{\Delta}{\pi})} \qquad (3)$$

From both theoretical and experimental work, the term $\frac{\Delta}{\pi}$ has been estimated to be several orders of magnitude less than $\frac{\pi}{\theta}$. Thus, the transfer function can be further simplified to that of a first order system:

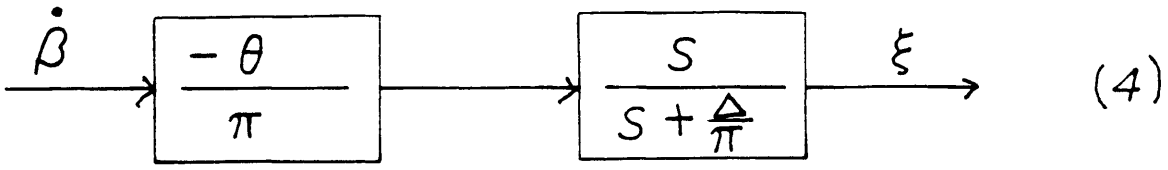

(4)

This transfer function indicates that the semicircular canals act as a high pass filter to head angular velocity.

To summarize, the ring of endolymph develops an angular velocity proportional to angular acceleration of the head. Although cupula deformation is initially proportional to head velocity, the deformation decays to zero due to cupula stiffness. Afferent nerve impulses from the canals, are approximately proportional to cupula deformation, ignoring adaptation affects and other nonlinearities.

The semicircular canals provide an estimate of head velocity which inputs to the oculomotor system. Optimally, it should move the eyes as far as the head, though in the opposite direction. However, if the head turns more than about thirty degrees, the eye globe will rotate to its full range of motion. It must then quickly reset, or "beat", in the direction of head movement to the opposite side of the eye socket to continue tracking a target. The beating motion is called a fast phase movement and is one example of a general type of eye movements called "saccades." The tracking motion is called a slow phase movement. A typical nystagmus eye position in time resembles a saw tooth wave with alternating fast and slow phases.

The sign of fast phase velocity is the negative of the sign of slow phase velocity, the amplitude of fast phase velocity is much greater than the amplitude of slow phase velocity, and the duration of a fast phase movement is much less than the duration of a slow phase movement. The mean angular position of the eyes during nystagmus is approximately zero.

2.2 Per rotatory and post rotatory nystagmus

Consider the effect of a square pulse angular velocity applied to the head, as shown in Figure 2.2.1.

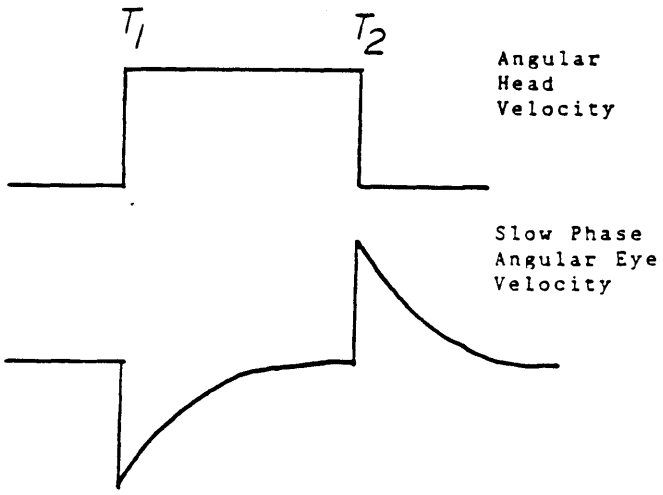

Effect of square pulse angular velocity applied to the head

Fig-2.2.1

At time T1, an acceleration impulse deforms the cupula, which then decays back to its resting position. The vestibular system drives the slow phase eye velocity with a characteristic time constant and gain. Slow phase eye movements are in the opposite direction of head movements to keep a target in view.

At time T2, eye movements have stopped and the subject feels that he

is not rotating. However, the acceleration impulse at time T2 drives slow phase movements in the opposite direction as before and the subject feels that he is rotating even though he remains still. Eye movement during head rotation is referred to as per rotatory nystagmus. Eye movement after head rotation is referred to as post rotational nystagmus or a post rotatory vestibulo-ocular reflex (PVOR).

2.3 The central velocity storage element

Experiments which measured afferent nerve signals from the semicircular canals of monkeys have suggested that the dominant time constant of the monkey cupula is about five seconds (Goldberg and Fernandez, 1971). Assuming human and monkey vestibular physiology is similar, cupula deformation alone probably does not drive slow phase eye velocity because human post rotatory slow phase eye velocity decays with an apparent time constant of about twenty seconds. (Malcolm, 1973)

Robinson (1977) and Raphan and Cohen (1985) have attempted to explain the apparent stretched time constant with an element that integrates afferent canal signals before they reach the oculo-motor system. Although anatomists have not conclusively identified such an element, Raphan and Cohen hypothesize that there is a central velocity storage element which holds an estimate of angular head velocity.

The phenomenon of optokinetic after nystagmus supports the theory of a central integrator. A moving visual field will induce smooth eye tracking movements. However, the tracking continues even after the scene stops, suggesting that the moving field charged the state of the integrator.

Figure 2.3.1 shows a sketch of the hypothesized states of the

horizontal canal, the central integrator, and the oculomotor system during a PVOR.

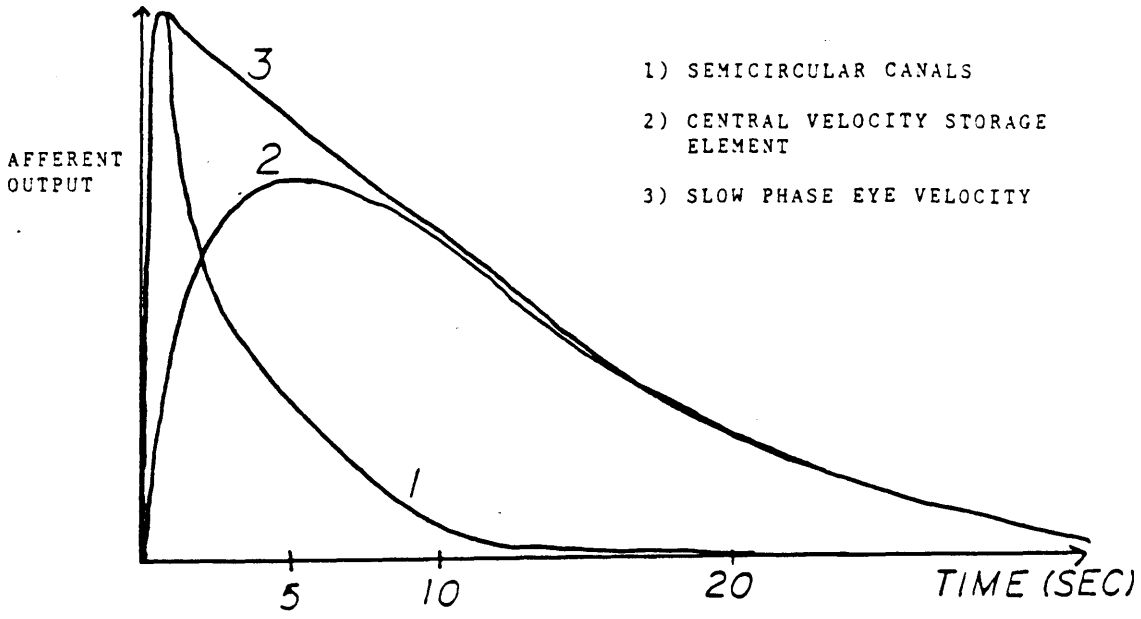

States of vestibular organs in response to a step head angular velocity

Fig-2.3.1

At time 0+, the cupula deforms. The afferent output decays quickly, but this signal charges the the central integrator. If the oculomotor system receives the outputs of both the canals and the integrator, then slow phase velocity is proportional to the sum of the states of the canal and the integrator and thus the effective time constant is stretched and approximates the leak time constant of the integrator after about five seconds.

Characterizing how this integrator affects slow phase angular eye velocity may be central to interpreting the results of this investigation. The state of the neural integrator may depend on

information from the gravireceptor.

2.4 Gravireceptor influence on the PVOR

The otoliths are organs located near the semicircular canals and provide an estimate of linear acceleration and head tilt. They contain calcium crystals which are embedded in a membrane. Linear acceleration shears the crystals over the membrane and stimulates hair cells beneath it. The otoliths can measure the angle of head pitch, or tilt, because the component of the gravity vector which shears the crystals over the membrane changes in magnitude with the angle of head position.

Consider the conflicting information coming from the semicircular canals and the otoliths when the head pitches forward during a post rotational test. The horizontal angular acceleration impulse to the head when it stopped rotating stimulated the horizontal canals. However, pitching the head forward translated the yaw axis into what was previously the roll axis. Thus, the canals inform the brain that the head is rolling about an earth horizontal axis, not yawing about an earth vertical axis. However, the otoliths measure a stationary gravity vector and do not confirm that the head is rolling. The brain receives information about body position from other organs, such as proprioceptors, so we cannot assume that the brain only weighs signals from the canals and the otoliths when forming an estimate of head angular velocity to properly drive slow phase eye velocity.

Presumably, the brain has learned over time that although the head constantly twists and pitches and rolls, the gravity vector probably does not change direction. Thus, during head tilt the brain probably weighs information from gravireceptors more than information from the

semicircular canals. Benson and Bodin's data supports the assumption because it shows that post rotational slow phase eye velocity decayed more quickly when the body pitched forward or back than when it remained upright. Slow phase eye velocity presumably reflects the vestibular system's best estimate of head angular velocity.

There is no gravity vector in weightlessness to stimulate gravireceptors when the body tilts, so it seems likely that the brain would learn to weigh signals from this organ less in space. If adaptation to weightlessness takes several days, it is possible that readaption to gravity when the spacelab crew returned to earth would not be instantaneous and adaptation effects could be measured in vestibular tests during the first few days postflight.

What adaptation effects are expected? There are several possibilities. If adaptation to weightlessness involved unweighting information from gravireceptors due to physical changes in vestibular structures, then slow phase eye velocity is not expected to decrease during head tilt as quickly postflight as it did preflight. However, if adaptation to weightlessness involved higher level learning instead of dramatic physiological changes, the brain may quickly ignore what it learned during weightlessness and instead weight gravireceptor information even more postflight than preflight because gravity would provide an overwhelmingly strong cue for body position.

Changes in the apparent head up time constant are harder to predict because it is not clear if gravity affects the physics of the semicircular canals. If on earth, the state of the central integrator is consistently influenced by gravireceptors, and if in space, gravireceptors are dormant, perhaps the brain would begin to mistrust the

state of the integrator because it would not normally change with head movements, as it would on the ground. Perhaps cupula afferent signals would be weighted more than on the ground compared to central integrator afferent signals, and the time constant of slow phase velocity would approach more the short time constant of the cupula. The brain might also learn to trust the visual system for cues about body position more in space than on earth because the vestibular system would instantly give different information from what the brain has learned to expect on the ground. Thus the brain may increase the leak rate of the central integrator because the brain does not want to hold what it is learning to perceive as inaccurate information. This would also make postrotatory slow phase velocity decay more quickly postflight than preflight.

2.5 Modeling the tilt suppression of nystagmus

Figure 2.5.1 show two suggested block diagrams to model the semicircular canal-gravireceptor-oculomotor system (Oman, personal communication). They were based on the model of Raphan and Cohen, but leave out other blocks relating to the optokinetic tracking system.

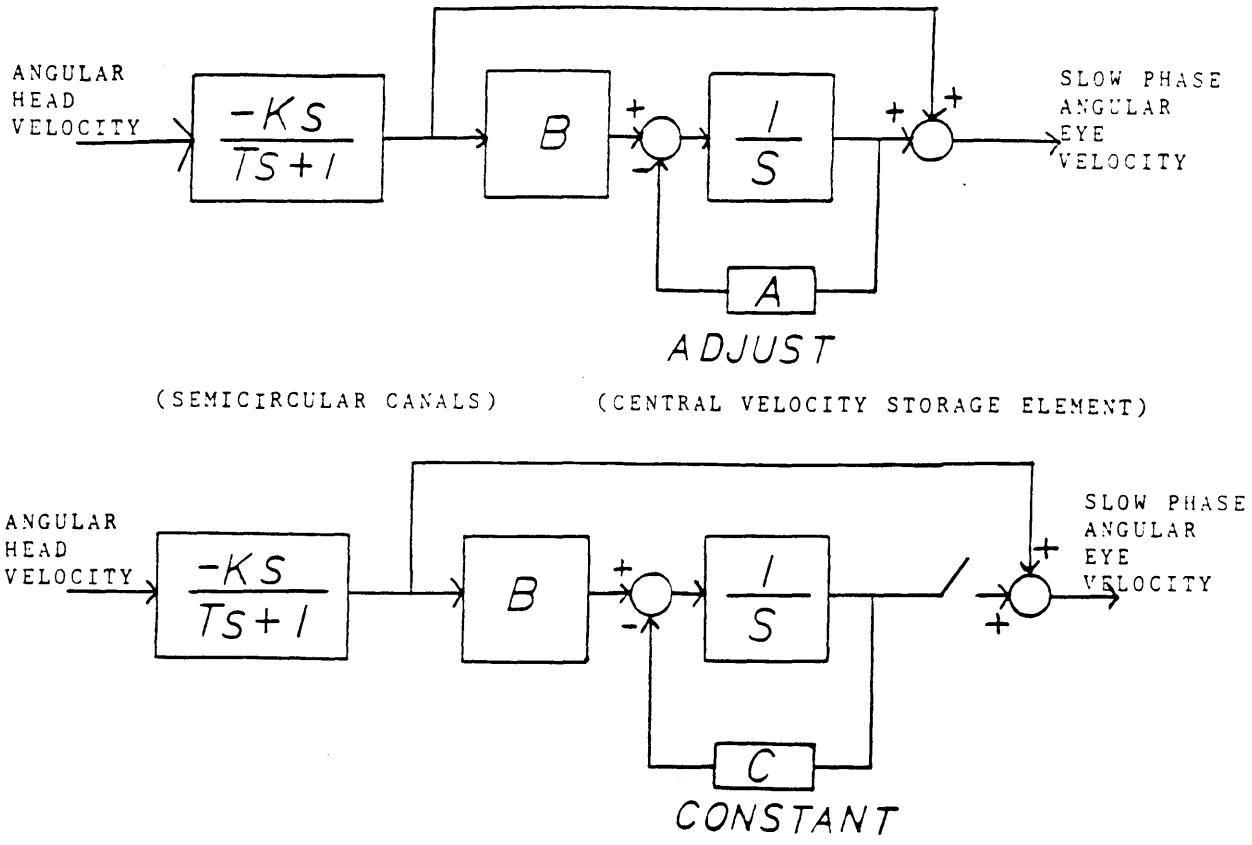

Canal-otolith-oculomotor system
Models
Fig-2.5.1

In each model, angular head velocity is high passed filtered through the dynamics of the cupula. Although the afferent canals signals go directly to the cupula in the feed forward path, a fraction of them input to the central integrator, which holds the state of the cupula and outputs to the oculomotor system. Thus the oculomotor system receives a sum of inputs from the canals and from the integrator. Notice that the integrator in each model has some leak rate through a negative feedback loop.

The two models differ in the way gravireceptors are hypothesized to affect the integrator state and its connection to the oculo-motor system.

In the top model, gravireceptors change the leak rate of the central integrator by adjusting the gain of the feedback element. In the bottom model, gravireceptors gate the signal of the central integrator away from the oculomotor system.

These models predict different time course rotational slow phase eye velocity both when the head tilts forward and when the head is brought upright again. The implications will be discussed later.

Chapter 3

Experimental Procedure.

Vestibular experiments were conducted at the NASA Dryden Flight Research Facility at Edwards Air Force Base, California by Oman and colleagues. EOG signals were recorded in analog form on FM magnetic tape. The data was digitized in the M.I.T. Man-Vehicle Lab by Eve Riskin. She used a PDP-11 computer which was manufactured by the Digital Equipment Corporation and an A/D program called SPARTA Lab Applications-11 which was also a marketed by DEC. Most of the work for this thesis comprised preparing and stripping the slow phase eye velocity from a raw nystagmus signal and then analyzing the experimental data. The experimental protocol proceeded as follows:

Identical tests were performed preflight and postflight. Six astronauts were tested preflight. Four of those six flew on the mission and were tested postflight. Subjects were tested on five separate days before the flight. The preflight tests were performed on days -151, -121, -65, -43, -10 days prior to launch. Post flight tests were performed on the flight crew three times after landing on days +1, +2, and +4.

The same protocol was followed for each subject on each day. The subject sat upright in a chair which could rotate about the vertical axis. Surface electrodes were placed on the skin beside the eyes to record vertical and horizontal eye movements, although horizontal eye movements were only of interest to this investigation. Subjects were blindfolded, but were told to keep eyes open during a test. Conversation and mental arithmetic were used to keep subjects alert.

A subject with the head upright was given a step angular velocity of 120 degrees per second in the clockwise direction for 60 seconds. The chair was then stopped within 1 second. Eye movements were analyzed for 45 seconds from the time the chair began to decelerate. These eye movements are referred to as the post rotational vestibular ocular reflex (PVOR). One minute after the chair stopped, the same procedure was repeated in the counterclockwise direction. This test will be referred to as a "head up PVOR."

Next, one minute after the chair stopped rotating counterclockwise, it was again brought up to speed in the clockwise direction to start "tilt suppression" experiments. When the chair stopped, the operator started counting on the second: 0-1-2-3-4-"down"-6-7-8-9-"up". At 5 seconds, the subject tilted his head down approximately 90 degrees and did not bring it back up until the operator counted to 10. As before, eye movements were analyzed for 45 seconds from the time the chair was commanded to stop. One minute after the stop, the same procedure was repeated in the counterclockwise direction. This test will be referred to as a "tilt suppression" or "head down PVOR."

Additional tests were then performed as part of a different investigation. The EOG gain was calibrated immediately before the first head up PVOR test, before the first tilt suppression test, and after the last tilt suppression test.

To calibrate EOG gain, a subject stared at a target directly ahead and the operator zeroed the DC component of the EOG amplifier output voltage. It was necessary to determine how many millivolts were recorded per angle of eye gaze. Keeping the head still, the subject then looked at targets to the left and to the right which were strategically placed

to require a 10 degree gaze angle. The surface electrodes measured a voltage proportional to a component of the corneo-retinal potential across the eye globe and thus proportional to angular eye position.

The EOG gain was calculated with eyes open, but the magnitude of the corneo-retinal potential changed as the eyes dark adapted when the subject put on the blindfold. Therefore the EOG gain was calibrated approximately every four minutes. EOG gain was interpolated between calibrations for each vestibular test.

Chapter 4

Data Processing

4.1 Overview of data processing

Five steps were required to prepare eye movement data recorded during a vestibular test for analysis.

1) Angular eye position was recorded by Oman at Dryden as a raw EOG signal.

2) The EOG signal was digitized at 100 Hz by Riskin at M.I.T.

3) A computer algorithm developed by Massoumnia at M.I.T. stripped its best estimate of slow phase eye velocity from the EOG signal.

4) Corrections of slow phase velocity were made by hand by the author with an interactive screen graphics program by DEC called SPARTA when the algorithm failed to perform adequately.

5) The data was transferred to a second PDP-11 computer where slow phase velocity signal was resampled to 4 Hz. Data was then transferred to an Apple IIc computer for statistical analysis using the program STATSPLUS (Human System Dynamics, Inc). Data was plotted using a version of DOTPLOT (CMI-Cascade, Inc) modified by Brian Rague.

Work for this thesis involved steps 3, 4 and 5.

4.2 Detection of slow phase movements

The top of Figure 4.2.1 shows a typical EOG nystagmus saw tooth shaped signal that was recorded during this investigation.

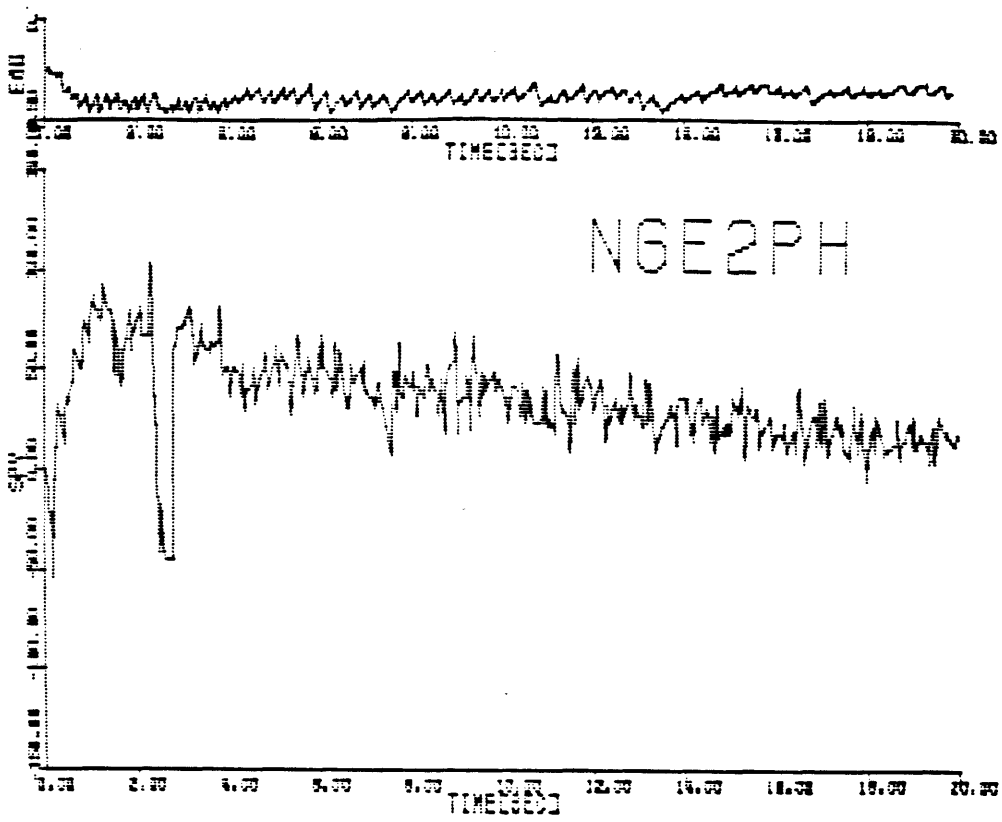

Typical output of Massoumnia algorithm

Fig. 4.2.1

It represents angular eye position vs. time. Below it on the graph is the output of the Massoumnia algorithm which showed an estimate of slow phase angular eye velocity vs time.

The algorithm first differentiated the angular position signal to get angular velocity. It then used a complex set of rules to classify movements as either slow phase or fast phase which involved relationships between the magnitude and sign of eye position, velocity, and acceleration. Those movements which it classified as fast phase were replaced with a linear interpolated signal between adjacent slow phase

movements. To better understand how the Massoumnia algorithm worked, observe Figure 4.2.2.

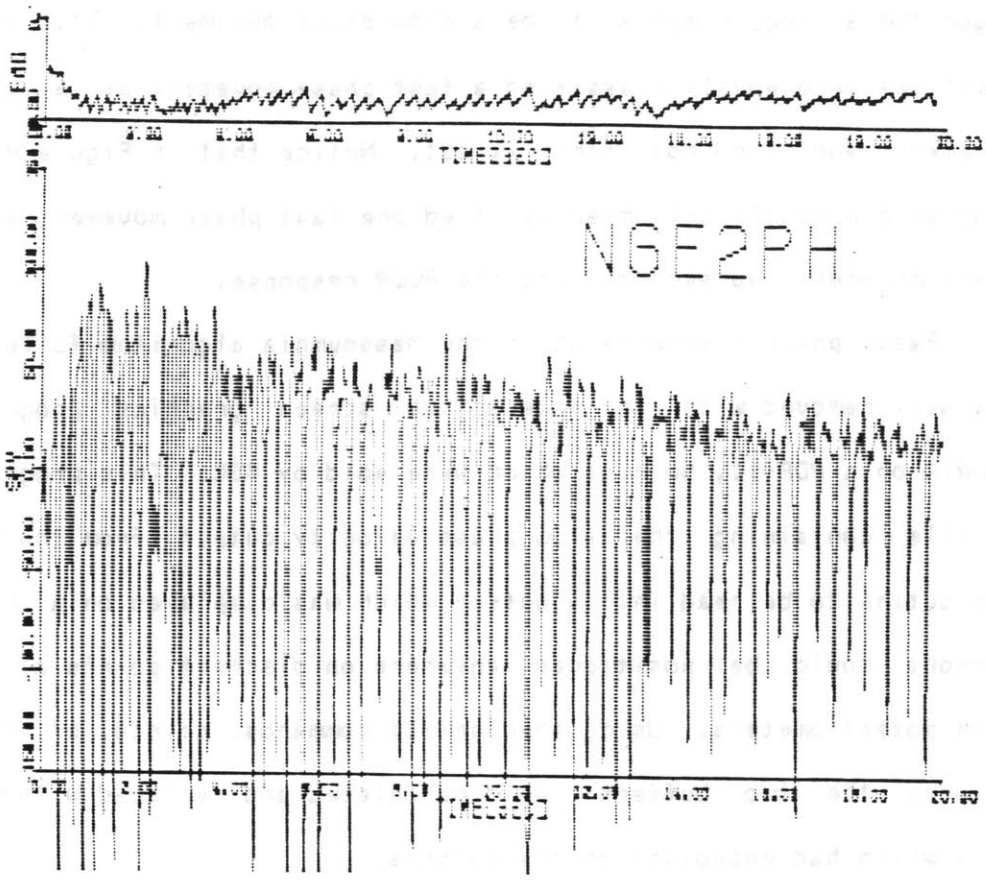

EOG and raw eye velocity plotted vs time

Fig 4.2.2

The top signal is the raw EOG signal which represents raw eye position vs time. The bottom signal represents an intermediate step of the program and would not normally be seen by someone using the algorithm. The bottom signal represents raw angular eye velocity vs time. This signal contains both fast and slow phases. The program examined this signal and stripped out those movements which it classified as fast phase, interpolating between adjacent slow phase movements to give the

estimated slow phase eye velocity signal that was shown in Figure 4.2.1.

It is possible that a fast phase movement can satisfy all the algorithm's requirements to be a slow phase movement. Thus the program sometimes erroneously classified a fast phase movement as a slow phase movement and did not strip it out. Notice that in Figure 4.2.1, the program apparently only misclassified one fast phase movement as a slow phase movement two seconds into the PVOR response.

Fast phase movements which the Massoumnia algorithm failed to strip out were removed with an interactive screen graphics program called SPARTA on a PDP-11, both of which were sold by DEC. This program allowed a file containing the slow phase velocity output from the Massoumnia subroutine to be read into a buffer which was displayed on a CRT. Two cursors could be positioned anywhere on discreet points of the signal with potentiometers. Using appropriate commands, points of the signal between the two buffers could be deleted and replaced with a straight line which had endpoints on the cursors.

Thus, SPARTA provided a way to linearly interpolate between two portions representing slow phase eye velocity over portions representing fast phase eye velocity which the program failed to delete. Because the deleted part of the signal was replaced with a straight line, the interpolation made that part of the slow phase angular eye acceleration appear constant in time.

As mentioned before, slow phase angular eye velocity in response to a step head angular velocity is approximately a decaying exponential. However, during the time up to one or two seconds in which fast phase movements were stripped out with SPARTA, slow phase velocity was approximately constant.

Figure 4.2.3 shows the same signal in Figure 4.2.1 after Sparta was used to remove a a fast phase movement in the slow phase velocity record profile.

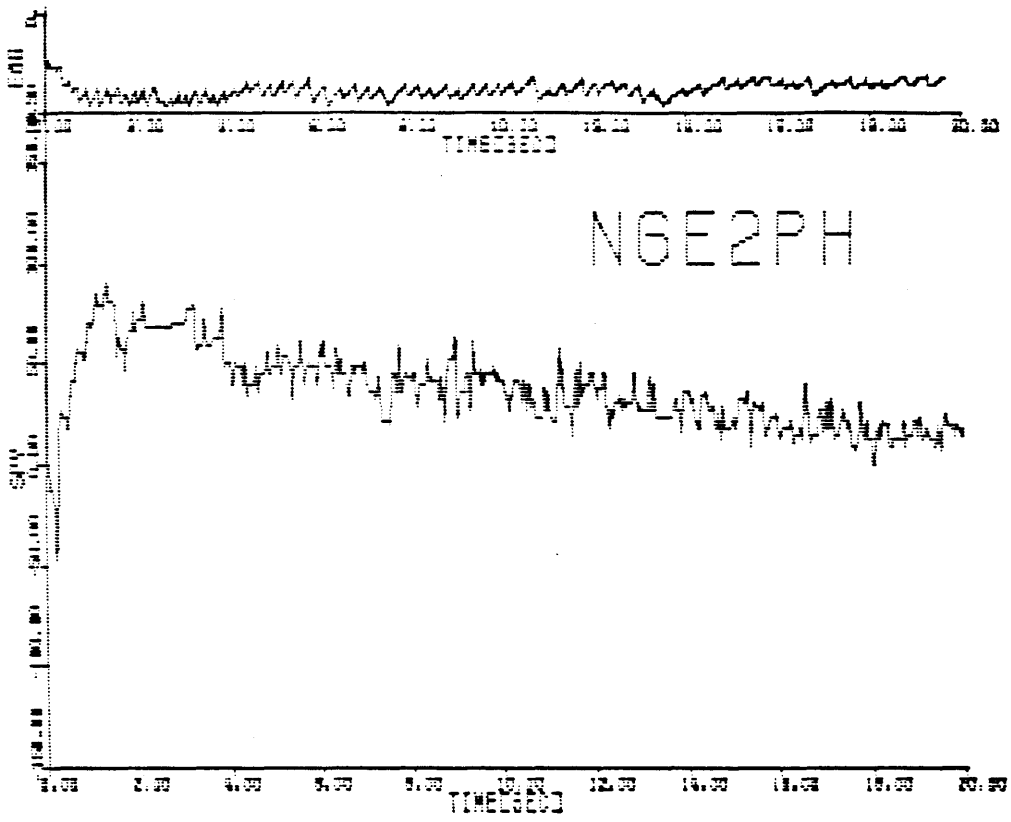

EOG and corrected slow phase velocity plotted vs time

Fig 4.2.3.

Cursors were positioned at the beginning and the end of the fast phase movement at two seconds into the record. SPARTA deleted the data points between the cursors and performed a linear interpolation between. After records were processed with Sparta, they were resampled from 100 Hz to 4 Hz to give a signal resembling that in Figure 4.2.4

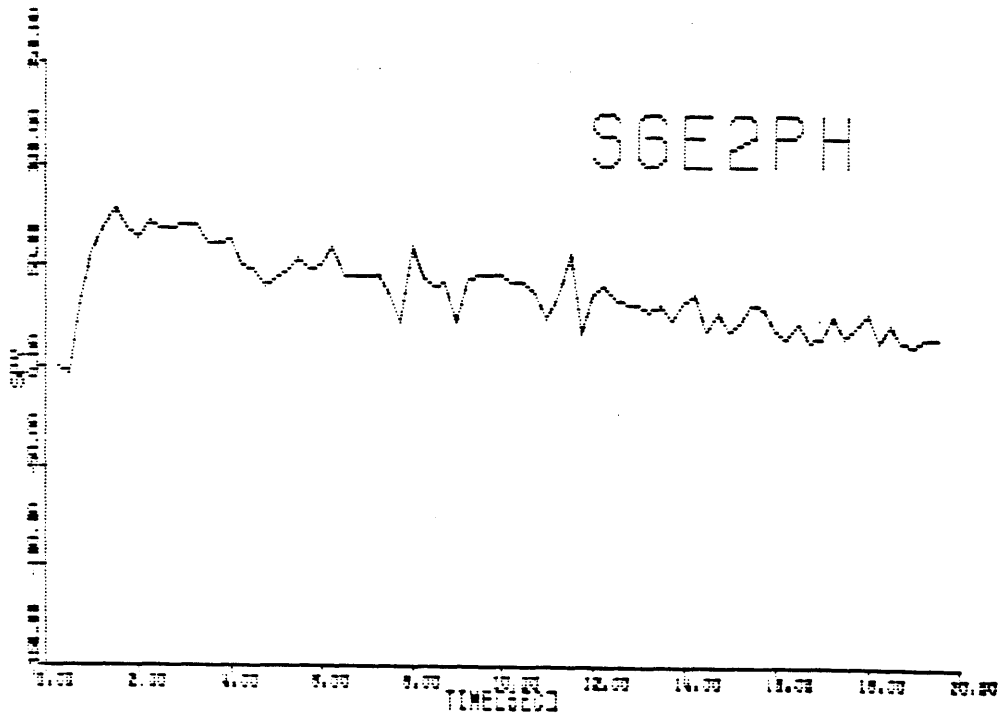

Slow phase eye velocity sampled at 4 Hz.

Fig 4.2.4

4.3 Criteria for correcting mistakes of the algorithm

Fast phase movements not removed by the Massoumnia algorithm had to be manually stripped out with SPARTA because data analysis would involve averaging across files. Misclassified fast phase movements such as those shown in Figure 4.2.2. would bias the average too low and greatly increase the variance for the slow phase velocity for a particular point in time. Missed saccades were manually stripped out with guidelines which were consistently followed:

1) When slow phase velocity was high (greater than about 60 degrees per second), the EOG signal contained high nystagmus beat frequency, low amplitude eye movements. Analog filters in the recording instrumentation, and digital filters in the algorithm to reduce high frequency noise, rounded out the high frequency fast phase movements to

make them appear as slow phase movements to the algorithm. Thus the program passed these fast phase movements instead of interpolating over them. In this case when the human eye could clearly separate fast phase movements from slow phase movements in the EOG signal, but the algorithm failed to do the same, the fast phase movements were manually removed. As the experimental procedure will later describe, slow phase velocity was highest at the beginning of the vestibular test. Thus, the algorithm failed in this respect here the most.

2) The algorithm sometimes detected a saccade, but failed to retrace the fast phase movement back to its start before interpolating across it. Figure 4.3.1 contains a schematic illustration of this type of error.

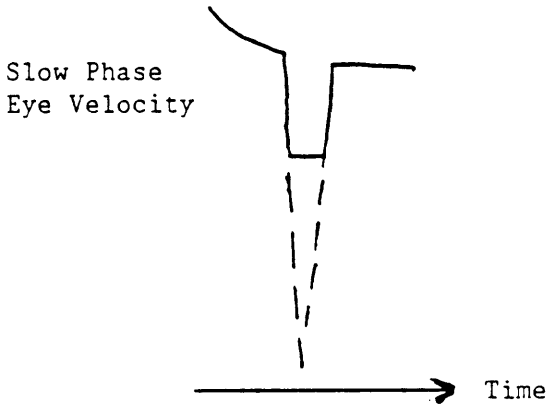

Schematic of a
poor interpolation

Fig-4.3.1

The remaining part of the saccade was manually removed if its amplitude was visibly greater than the amplitude of the random noise of the signal.

3) DC drift in the recording equipment forced the operator to sometimes adjust the DC offset of the recording instrumentation during a test. If the algorithm misinterpreted this glitch as a slow phase

movement, it was manually removed.

4) If the signal to noise ratio of an EOG signal was not constant in time, the algorithm sometimes completely failed in some sections of a test and worked adequately in others. Up to two seconds of worthless noise in the velocity signal was manually interpolated out with the interactive screen graphics program if a clean slow phase velocity signal was evident on either side.

5) In slow phase eye velocity profiles of tilt suppression tests, the velocity signal often transiently dropped at 5 and 10 seconds. Remember that subjects tilted the head forward at 5 seconds and brought it upright again at 10 seconds. It is not known whether this apparent drop in the velocity signal was due to an artifact of the recording instrumentation or a true velocity transient. One possible technical artifact may be that pitching the head forward and back caused the eyes to transiently roll up and down in the head, which transiently changed the component of the corneo-retinal potential recorded by surface electrodes near the temples. Electrode motion artifact may have also contributed. Brief transients occurring at 5 at 10 seconds were removed.

4.4 Criteria for discarding files

The performance of the program depended most importantly on the signal to noise ratio of the EOG signal. Figure 4.4.1 shows one file for which the program interpolated the slow phase velocity across almost all saccades. The top signal is the raw EOG signal which represents angular eye position vs time. The bottom signal represents the slow phase eye velocity vs time of that signal. Figure 4.4.2 shows one file in which noise in the EOG signal cause the algorithm to fail frequently.

The program correctly identified and stripped out approximately 50% to 95% of all saccades depending largely on record noise level. This performance varied greatly between subjects. Some subjects had a consistently low corneo retinal potential and thus had a high signal to noise ratio which caused the algorithm to fail. Researchers who plan to use this program might consider choosing test subjects with a high corneo-retinal to extract optimal performance form the Massoumnia algorithm.

In this investigation, 145 EOG signals from separate vestibular tests were input to the stripping program. 21 (13%) were not used for data analysis. Although files were discarded from all subjects, profiles of responses from subject 1 were discarded more than the others because he had a consistently low EOG gain. Files were discarded for the following reasons.

1) A relatively noiseless EOG signal sometimes became extremely noisy, suggesting that an electrode lost good contact with the skin.

2) An EOG signal had such a constantly high signal to noise ratio that the algorithm completely failed to strip slow phase eye velocity.

3) The beginning of a velocity profile from a PVOR test showed no eye movement at all. This indicated that the the beginning of the profile was missed when data was transferred from FM tape to digital media. Some profiles showed a low initial response, as opposed to no initial response. It was believed that subjects with a high initial slow phase velocity for most PVOR tests who had virtually absent responses to stopping the chair were likely sleepy during that portion of the test. These files were discarded only if the response profile was markedly atypical. Three records were discarded that contained no eye

movements. Three more were discarded because the subject was sleepy.

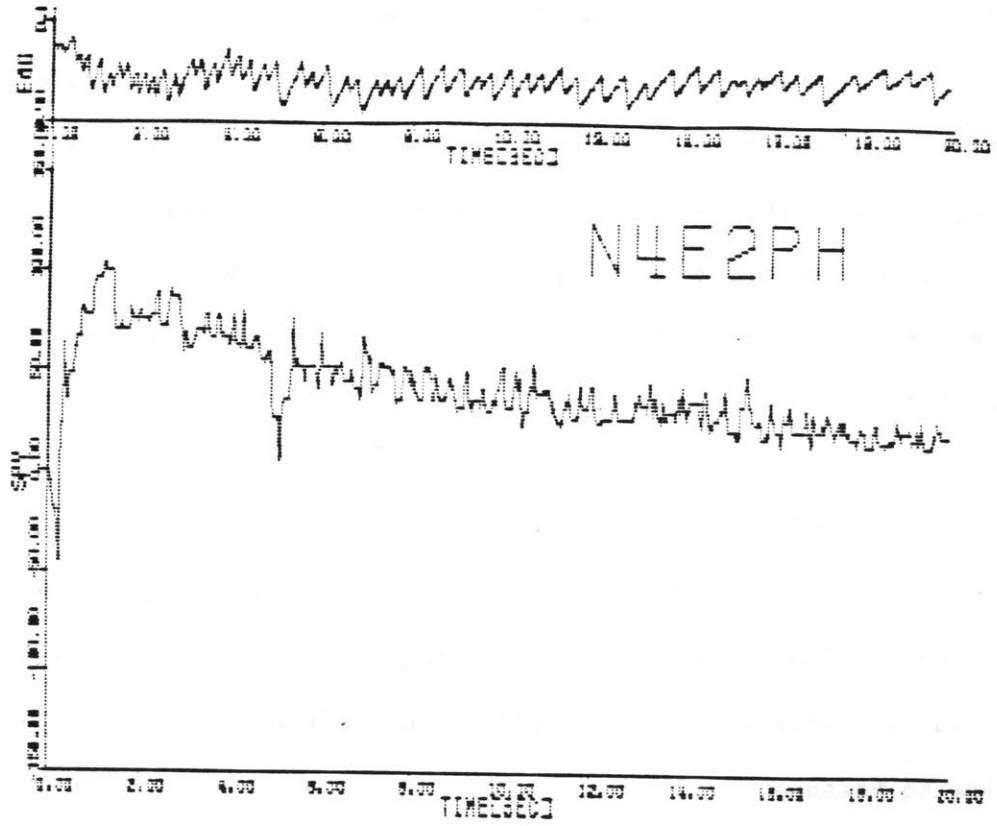

Fig. 4.4.1 High performance of algorithm

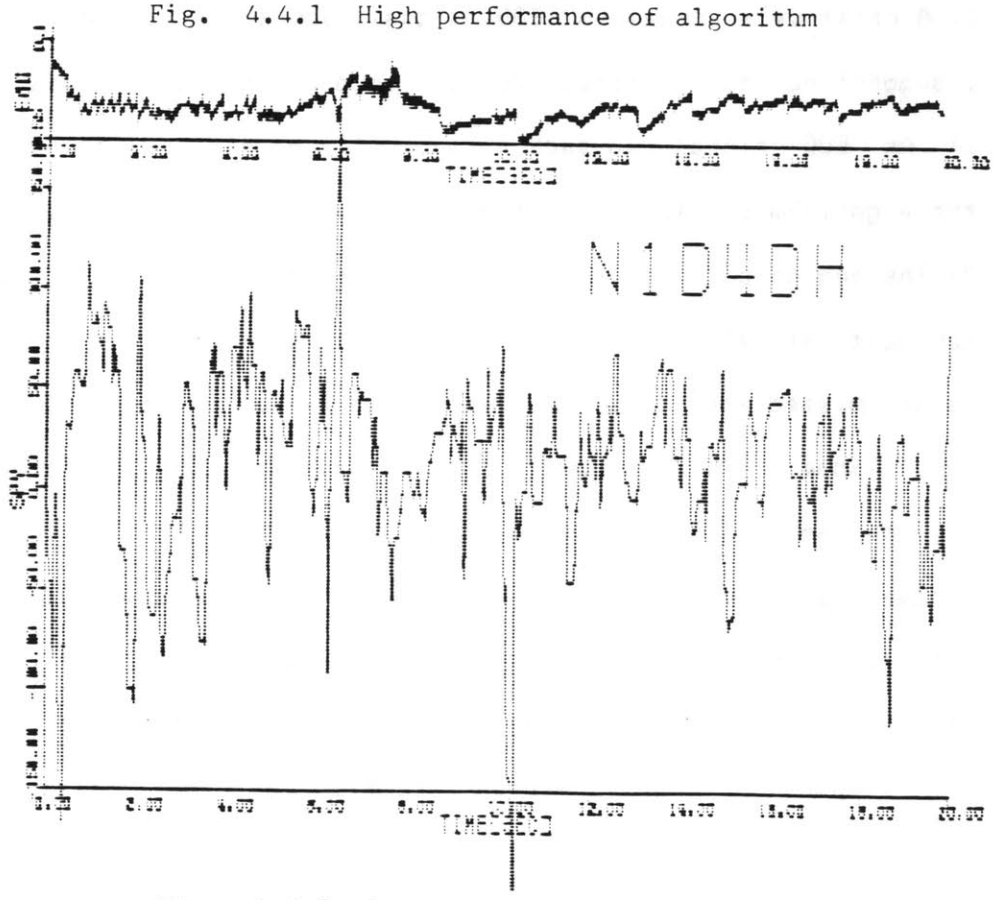

Fig. 4.4.2 Low performance of algorithm

Chapter 5

Strategies For Analyzing The Data

5.1 Two statistical methods for analyzing PVOR data

Remember that the primary goal of this experiment was to characterize the pre and post spaceflight head up and head down slow phase eye velocity profiles of the post rotational vestibulo-ocular reflex. A general method was needed to test if two PVOR responses were statistically significantly different. The chi-squared test was used to test if two mean responses were significantly different without fitting those responses to a model. A method was also needed to test what fitted model parameters, if any, made two PVOR responses different. A t-test was used to test if the parameters of model fits were significantly different.

Before proceeding with a discussion of the statistical analysis performed for this project, it is necessary to outline the circumstances in which the analysis was conducted. This investigation had to proceed within a strict schedule, and unexpected problems with computer hardware prevented the manipulation of much of the data which was required to perform the most comprehensive statistical analysis. A preliminary statistical analysis was performed with the intent of documenting possible changes in PVOR head up and head down responses preflight and postflight.

5.2 Combining clockwise and counterclockwise responses

Because identical tests were performed on each subject in the clockwise and counterclockwise directions, the number of sample responses

drawn from the population could be, in effect, doubled if subjects had identical responses in both directions. If responses in either direction were not similar, then tests in each direction would have to be analyzed separately. The chi-squared test was used to measure if a subject's post rotatory vestibulo-ocular reflex would have to be analyzed separately.

At Dryden, on each subject on each test day, head up PVOR tests to the left and right, and tilt suppression PVOR tests to the left and right were performed. Data was processed and eventually read into a two dimensional array of slow phase velocity from 0 to 37.75 seconds sampled at four Hz.

Each subject's head up PVOR responses during the five preflight test days in the clockwise direction were averaged. The head up PVOR responses in the counterclockwise direction were also averaged. The head down PVOR files in each direction were averaged. A sample variance of the slow phase velocity for each discrete point in time for each mean file was calculated. The sign of the slow phase phase velocity in the counterclockwise direction was inverted so that a chi-squared test could be performed on the mean responses in both directions.

A chi-squared value, χ^2 was calculated for clockwise vs counterclockwise head up tests, and for the clockwise vs clockwise head down tests according to the following formula: (Natapoff, personal communication)

$$\chi^2 = \sum_{i=1}^{N} \frac{(\overline{X}_i - \overline{Y}_i)^2}{\sigma_{P_i}^2} \qquad (5)$$

where $\sigma_{P_i}^2$ is the pooled weighted variance, $\overline{x}_i$ is the sample mean for time i of file x, $\overline{y}_i$ is the sample mean for time i of file y, and N is

the number of points in time which are compared.

$$\sigma_{P_i}^2 = \left[\frac{(N_x-1)\sigma_{x_i}^2+(N_y-1)\sigma_{y_i}^2}{N_x+N_y-2}\right]\left[\frac{1}{N_x}+\frac{1}{N_y}\right] \qquad (6)$$

where N_x is the number of records averaged into file x, N_y is the number of records averaged into file y, $\sigma_{x_i}^2$ is the variance of x_i, $\sigma_{y_i}^2$ is the variance of y_i. Chi-squared tables were obtained from Statistical Methods, by Snedecor and Cochran. If $\chi^2 = N$, then the average squared difference between the mean slow phase velocities foe each point in time is equal to the pooled variance of that point in time, and thus the two responses are significantly different. Chi-squared tables give 95% confidence levels for the chi-squared value of each N. If n=100, then the null hypothesis that two curves are identical is disproved with 95% confidence when χ^2 is greater than 124. The slow phase velocity values for 100 discrete points in time from 2 to 27 seconds were compared in the chi-squared tests. The accuracy of the first two seconds was suspect because of performance problems with the algorithm, as described earlier. After 27 seconds, the slow phase velocity had decayed close to zero, where factors such as alertness and adaptation became significant. Also, chi-squared tables with N=100 were the largest located. The chi-squared tests were performed on the records at 100 Hz before they were resampled to 4 Hz.

The basis for the decision to average responses for a given subject in a given direction across test days to obtain an estimate of his mean response in that direction was that there was no trend, or learning curve in a subject over the preflight testing period. To test this assumption, chi-squared tests were performed on mean responses of the

population on a given day. Chi-squared tests did not indicate that the difference of the mean responses of the population were significantly different with 95% confidence between preflight testing days (1,3), (1,5) and (3,5). However, this test only was useful for testing if there was a preflight learning curve for the population. It said nothing about the possibility of learning curves within individual subjects. However, no trends were seen when the data was scrutinized by eye for individuals and the analysis proceeded, noting the possibility that individual trends may have affected the results of chi-squared tests which compared right vs left rotations per subject.

The head up PVOR χ^2 values for subjects 1 ,2 ,3 ,4 ,5 and 6 obtained by comparing mean preflight clockwise and counterclockwise directions were 123, 86, 68, 86, 334, and 374. It is was not suspected that every subject's PVOR responses would be similar in opposite directions, because asymetries are commonly observed in humans. However, the chi-squared test was used to examine which subjects had approximately similar responses in either direction. The results of the chi-squared test suggested that the difference between clockwise and counterclockwise preflight head up PVOR responses was significant with 95% confidence for subject 5 and 6. The X^2 value for subject 1 was borderline in proving that his responses were significantly different. Subject one had the noisiest EOG signals and the Massoumnia algorithm performed least well with him, so it is suspected that the algorithm exaggerated differences between the responses, and it was judged that the clockwise and counterclockwise head up PVOR tests could be averaged. Subjects 2 ,3 and 4 had similar preflight head up PVOR responses in either direction.

The preflight head down PVOR χ^2 values for subjects 1 through 6

were 124, 224, 114, 109, 303, and 401. Again, subjects 5 and 6 showed significant differences between the clockwise and counterclockwise directions and subject 1 was borderline. Subjects 3 and 4 had no significant difference in either direction. The chi-squared test on subject 2 indicated that the difference in the clockwise and counterclockwise responses was significant . However, the two mean responses appear very similar except for a few seconds where the signals transiently digressed. This may be explained by the fact that few numbers of test days were able to be averaged together for this subject. Subject drowsiness or algorithm failure during only one PVOR test were thought to have biased the mean responses in that direction. Because subject 2 did not have significantly different head up PVOR responses, it was decided that both his head up and head down PVOR files in either direction could be averaged with some justification.

Only 2 of the 6 subjects (#3,#4) showed no significant difference in preflight clockwise or counterclockwise head up or tilt suppression PVOR tests. Because subjects 5 and 6 did not fly on the mission, and it was observed that the their PVOR responses were not symmetric, their data was not examined again. It was suspected that algorithm examined slight differences in the directional responses of subjects 1 and 2. Thus the above analysis concluded that clockwise and counterclockwise PVOR responses could be averaged for individuals 1 ,2 ,3, 4, noting that it was possible that minor asymetries could have been present to some degree.

With the final goal to be able to average all preflight clockwise and counterclockwise responses for each day for each subject, the preceding chi squared analysis has suggested that:

1) The mean PVOR responses for the sample population as a whole changes little from day to day.

2) Clockwise and Counterclockwise PVOR responses were not materially different for each of the first four subjects.

Before justifying the utility of such a global average, it was first necessary to investigate the variance of the responses between individuals. For a more accurate way of examining the source of this variance, individual responses were fit to models. The results will be presented in the next chapter.

Chapter 6

Modeling Slow Phase Eye Velocity During A PVOR

In the most simple vestibulo-ocular model that does not account for the central integrator or adaptation effects, canal afferent signals drive slow phase eye velocity. The Steinhausen equation predicts that a step head angular velocity elicits slow phase velocity which has a profile resembling the response of a high pass filter with characteristic time constant and gain. The Raphan and Cohen model predicts that a PVOR response would better fit to a two time constant model. Oman and Young (1969) have shown that adaptation effects require a PVOR response to be fit to at least a three time constant model for more accuracy. However, before attempting to fit data to a complicated model, it was decided that the main features of nystagmus between 1 and 20 seconds could be adequately described by a two parameter first order model with a time constant and gain. Parameterizing head up PVOR responses with a gain and apparent time constant provides a way of testing if two mean responses differ mainly in the initial amplitude or in the rate of decay.

To provide a rough estimate of how well head up PVOR profiles would fit to a one time constant model, the mean response of all preflight head up PVOR responses was plotted + and - one standard error of the mean. (It was noted that clockwise vs counterclockwise responses could be different and that responses between subjects probably were not similar in detail.) This signal, which is shown in Figure 6.1.1, approximately looks like an exponential.

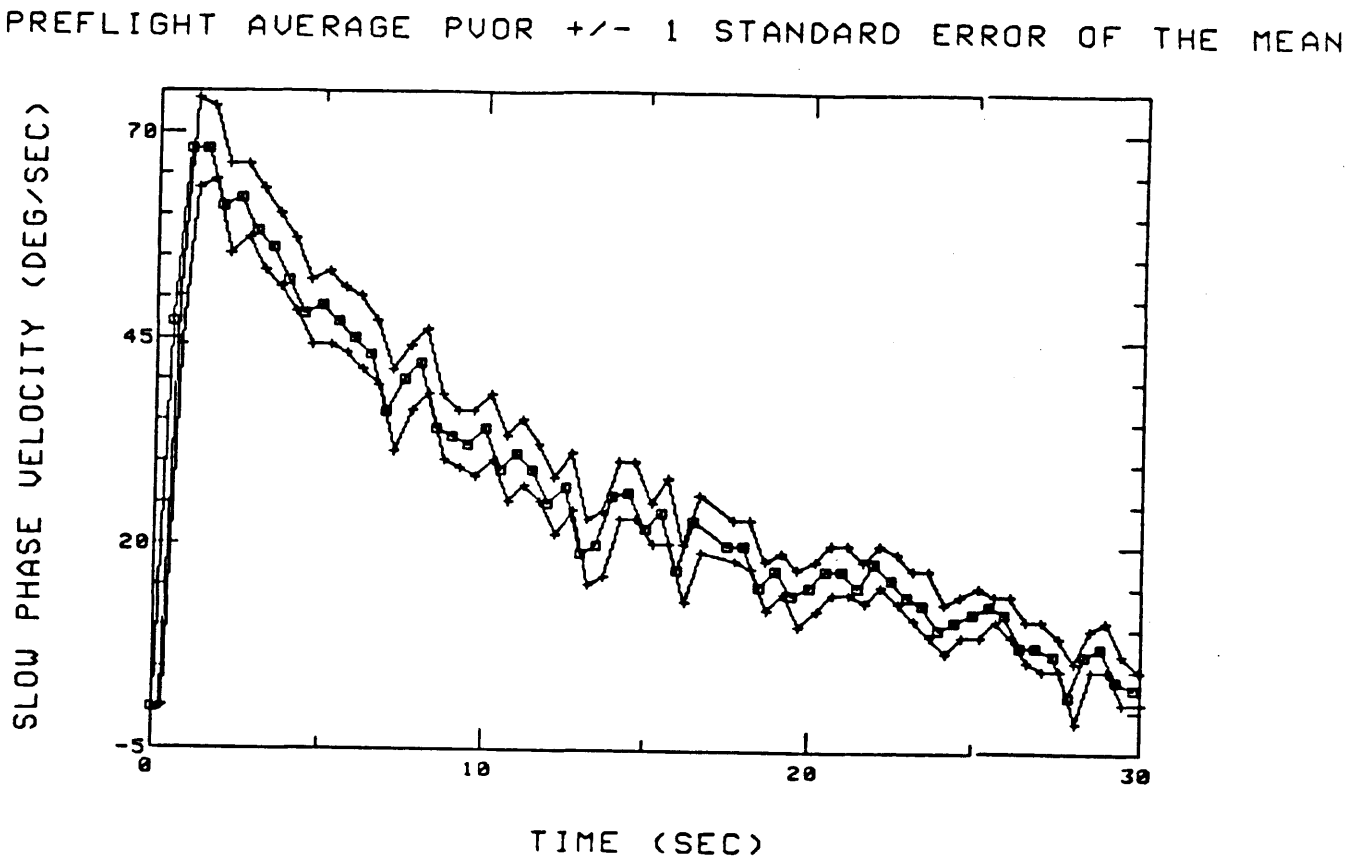

Fig. 6.1.1 Global preflight head up PVOR profile

If it truly were a decaying exponential, the natural log of the slow phase velocity plotted vs time would be a straight line. The intercept would equal the negative inverse of the time constant and the y-intercept would define some characteristic gain. Figure 6.1.2 shows a scatterplot of the natural log of the sample population's head up slow phase velocity vs time from 1 to 20 seconds.

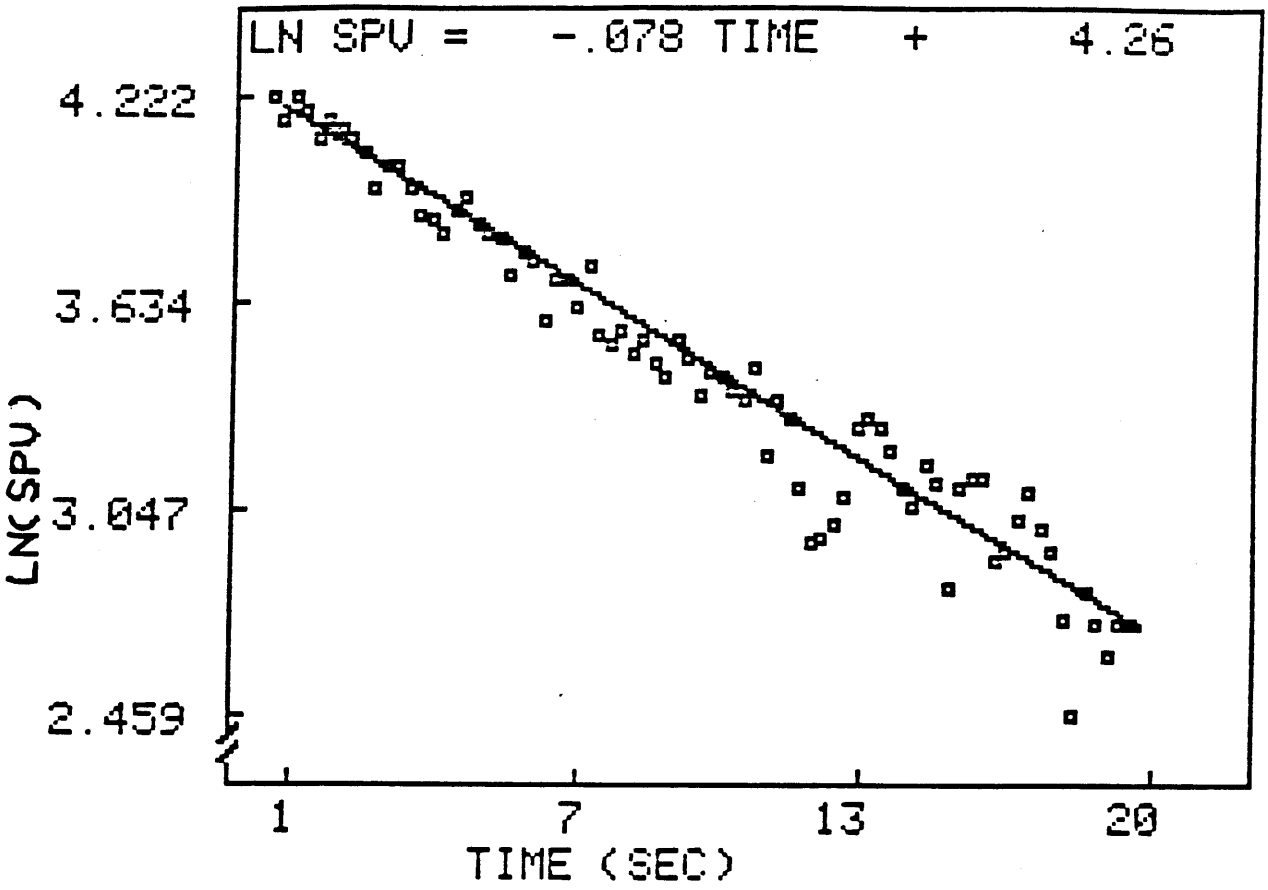

Fig. 6.1.2 Model fit of mean preflight head up PVOR

The line in the plot minimizes the sum of squares of the errors between the line and the points. This plot suggests that the data can be approximately parameterized to a one time constant model, at least for twenty seconds of a PVOR. It was known that the one time constant model for slow phase angular eye velocity would break down at some time during a PVOR because of adaptation effects (probably in the peripheral neuron) which create nystagmus in the opposite direction after 25 to 35 seconds.

Oman (1969) suggested that the time constant for these adaptation effects is about 80 seconds. Thus fitting the head up PVOR time constant to a 1 time constant model for twenty seconds was somewhat justified.

Chapter 7

Results

7.1 Mean PVOR Responses of Individuals

Chi-squared tests comparing mean responses of the 4 subject population for preflight test days 1, 3, and 5, did not prove that mean responses were significantly different at the 5% level. Thus there was no obvious trend in the responses over time of the population. It is possible that there were counterbalancing trends in individuals, but this is not likely because no individual trends were observed when examining individual responses with the eye. Preflight head up and tilt suppression tests were averaged across the five testing days for each of the four subjects to obtain a mean preflight head up PVOR response and a mean postflight tilt suppression PVOR response for each subject. These responses were fit to first order models by plotting the natural log of the slow phase velocity vs time from 1 to 20 seconds. The negative reciprocal of the slope then represented an apparent time constant and the inverse natural log of the y-intercept divided by 120 (the input step velocity in angular degrees per second) represented a gain. Table 7.1.1 shows the results of individual subject model fits.

SUBJECT	HEAD UP TIME CONSTANT (SEC) PREFLIGHT	POSTFLIGHT	HEAD DOWN TIME CONSTANT (SEC) PREFLIGHT	POSTFLIGHT	GAIN PREFLIGHT	POSTFLIGHT
1	7.4	4.9	7.7	3.2	.48	.48
2	13.9	7.1	8.7	4.8	.52	.58
3	16.7	11.2	3.7	1.3	.58	.75
4	11.1	13.9	3.1	3.0	.78	.59
Average	12.3	9.3	5.8	3.1	.59	.60
Standard Deviation	4.0	4.0	2.8	1.4	.13	.11

RESULTS OF MODEL FITS TO INDIVIDUALS

Table 7.1.1

The population preflight head up time constant +/- one standard deviation for individuals was 12.3 +/- 4.0. Head down time constants were calculated from the slope of the regression line for the tilt suppression tests by fitting the data from 5 to 10 seconds. The mean head down preflight time constant for individuals was 5.8 +/- 2.8 seconds. The mean gain was 0.59 +/- 0.13.

A chi-squared test on the first two days of head up post flight responses for the 4 subject population did not indicate that the mean response on day +1 was significantly different from the mean response on day +2. The response of the population on the third postflight day was significantly different from the responses of the first two postflight days. The head up and tilt suppression runs for the first two days postflight were averaged together, respectively, for individual subjects.

Post flight head up and head down time constants were calculated from model fits. The mean postflight head up time constant for individuals +/- 1 standard deviation was 9.3 +/- 4.0 seconds. The mean postflight head down time constant for individuals +/- one standard deviation was 3.1 +/- 1.4 seconds. The post flight gain was 0.60 +/- 0.11 These results are shown next to the preflight results in Table 7.1.1. Pre and post flight head up and head down, or nystagmus dumping, time constants are shown for individual subjects in bar graph form in Figure 7.1.2.

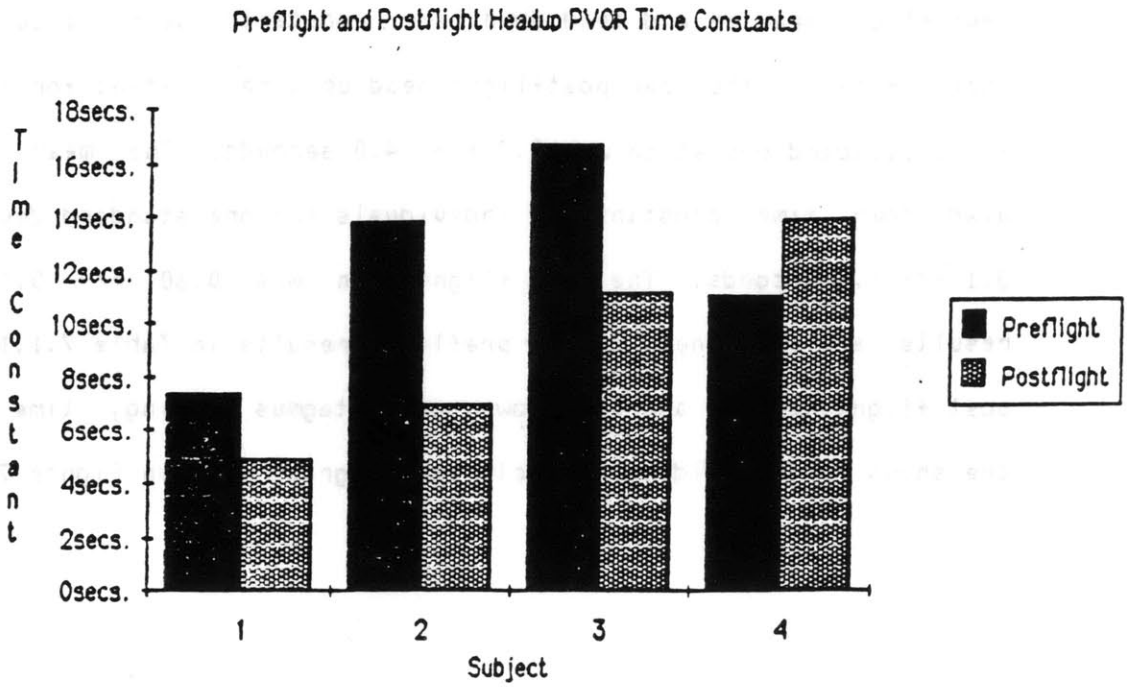
Preflight and Postflight Headup PVOR Time Constants
Time Constant
18secs.
16secs.
14secs.
12secs.
10secs.
8secs.
6secs.
4secs.
2secs.
0secs.
1
2
3
4
Subject
Preflight
Postflight

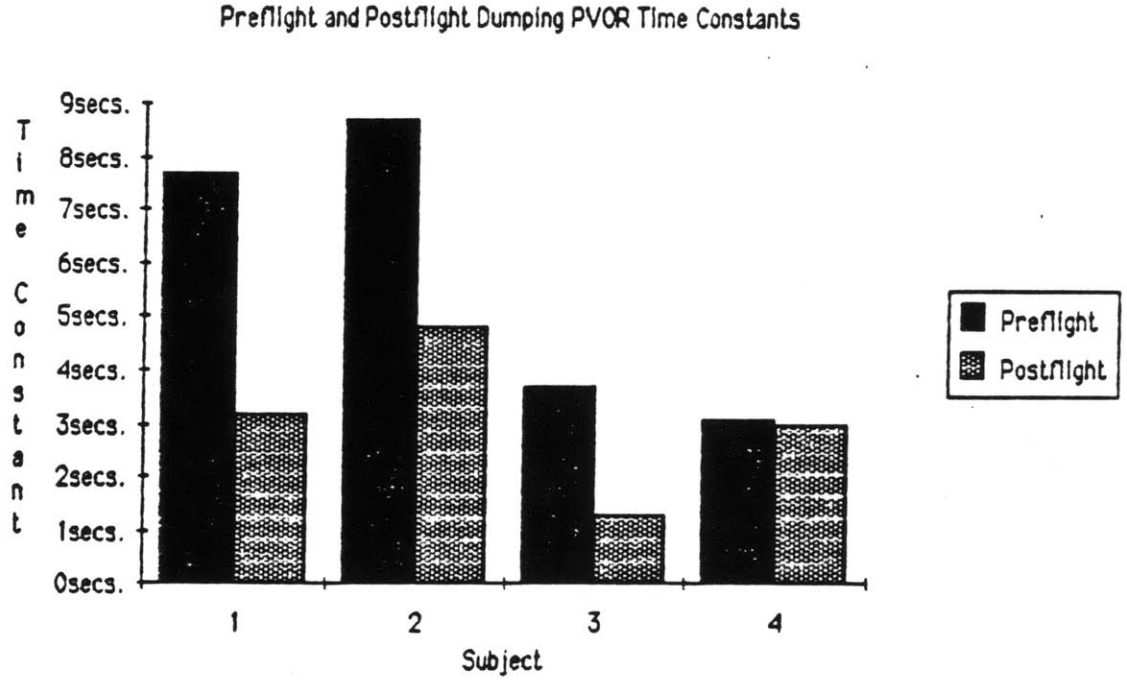
Preflight and Postflight Dumping PVOR Time Constants
Time Constant
9secs.
8secs.
7secs.
6secs.
5secs.
4secs.
3secs.
2secs.
1secs.
0secs.
1
2
3
4
Subject
Preflight
Postflight

Fig 7.1.2

Notice that the mean head up postflight time constant was less than the mean head up preflight time constant for subjects 1, 2, and 3. Subject 4 had a slightly higher mean postflight head up time constant than preflight. The mean postflight head down time constant appeared less than the mean preflight head down time constant for subject 1, 2, and 3. Subject 4's head down response appeared unchanged preflight to post flight. There appeared to be no significant trend in the PVOR gain preflight to postflight.

The preceding analysis across days for each subject has given an estimate of the mean preflight and post flight head up and head down time constants and gains for the sample population. We are interested in learning if living for 10 days in weightlessness caused the vestibulo-ocular system to adapt in ways that can be measured. As a first attempt to quantify the possible difference between preflight and postflight responses, independent sample t-tests were performed on the subject mean parameters of the apparent head up and head down time constants and the PVOR gain. However, neither independent or dependent sample t-tests disproved the null hypothesis with 95% confidence that there was no difference pre and post flight in the sample population's head up time constant, head down time constant or gain. The variance in the responses between subjects was too large for any statistically significant conclusions to be drawn about the changes in the mean pre and post flight responses of the population with a t-test analysis.

A chi-squared analysis comparing pre and post flight head up responses for individual subjects indicated that the responses of subject 2 and 4 were significantly different pre and post flight. However, the mean head up time constant of subject 2 was less postflight

than preflight. The mean head up time constant for subject 4 was greater postflight than preflight. A chi-squared analysis comparing pre and post flight head down responses for individual subjects indicated that responses for each subject were significantly different preflight and postflight. However, this result must be cautiously interpreted.

The chi-squared test was sensitive to any parameters of the response which might have changed preflight to postflight. The magnitude of the slow phase velocity at 5 to 10 seconds depends on the time constant and the gain of the response from 1 to 5 seconds. Thus although the chi-squared test indicated that the preflight and postflight head down time constants for each subject could not be superimposed on the same graph, the chi-squared test could not relate if this was due to a change in the gain, the head up time constant, or the head down time constant.

Figures 7.1.3-7.16 show the mean preflight and postflight head up and tilt suppression PVOR responses for individuals. The plots show post rotatory slow phase eye velocity vs time.

SUBJECT #1 PREFLIGHT PVOR WITH/WITHOUT TILT SUPPRESSION

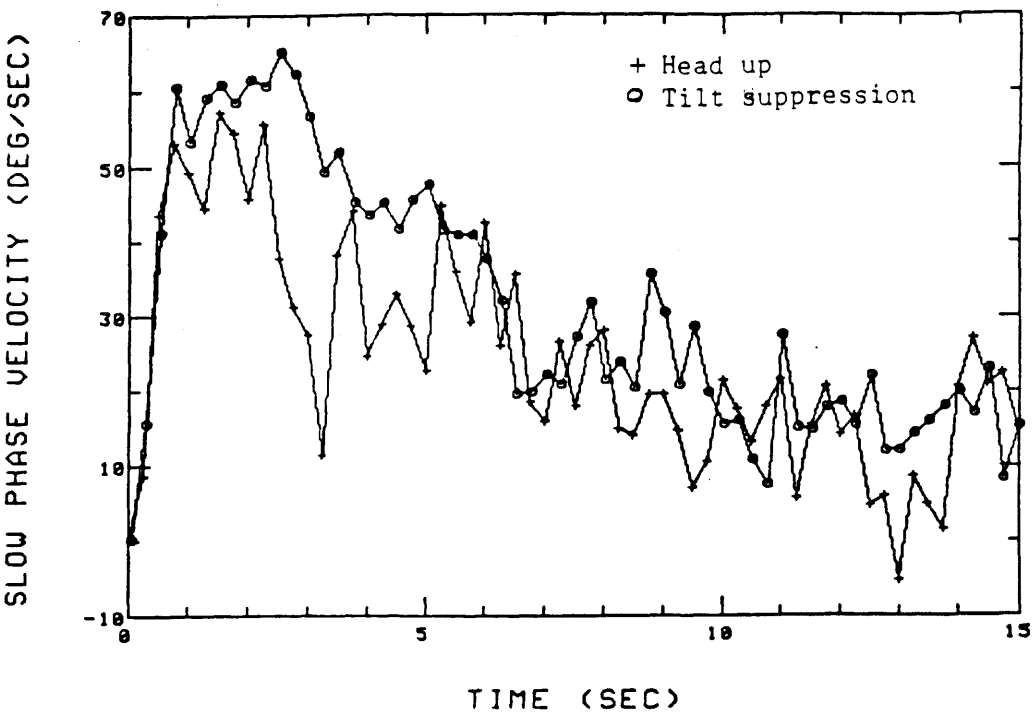

SUBJECT #1 POSTFLIGHT PVOR WITH/WITHOUT TILT SUPPRESSION

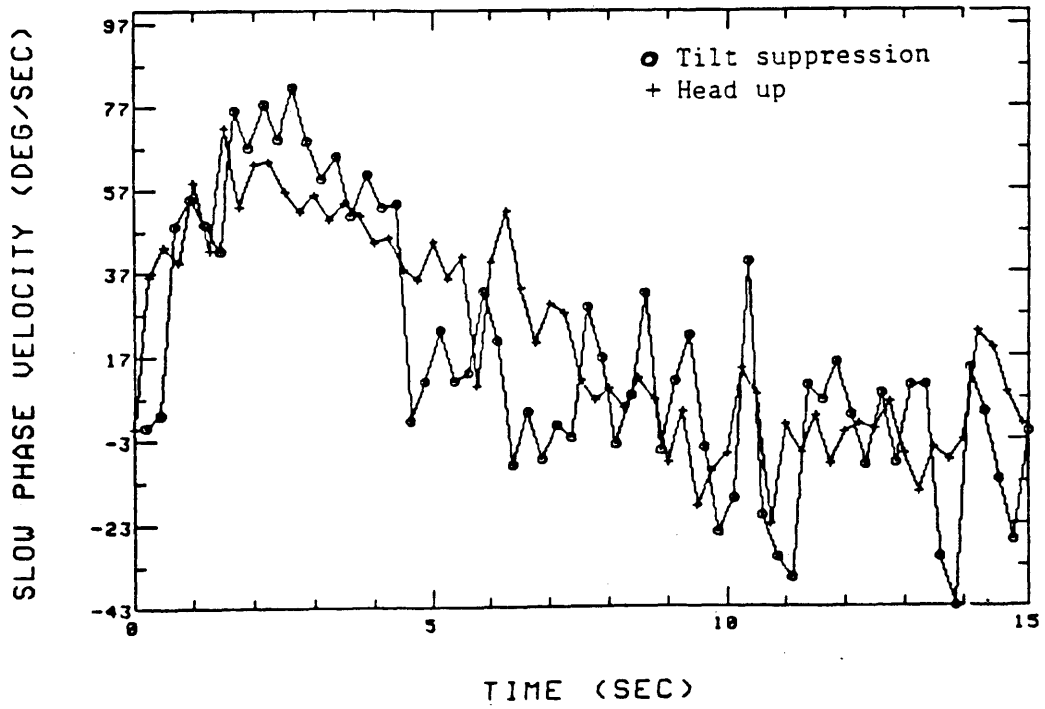

Fig. 7.1.3

SUBJECT #2 PREFLIGHT PVOR WITH/WITHOUT TILT SUPPRESSION

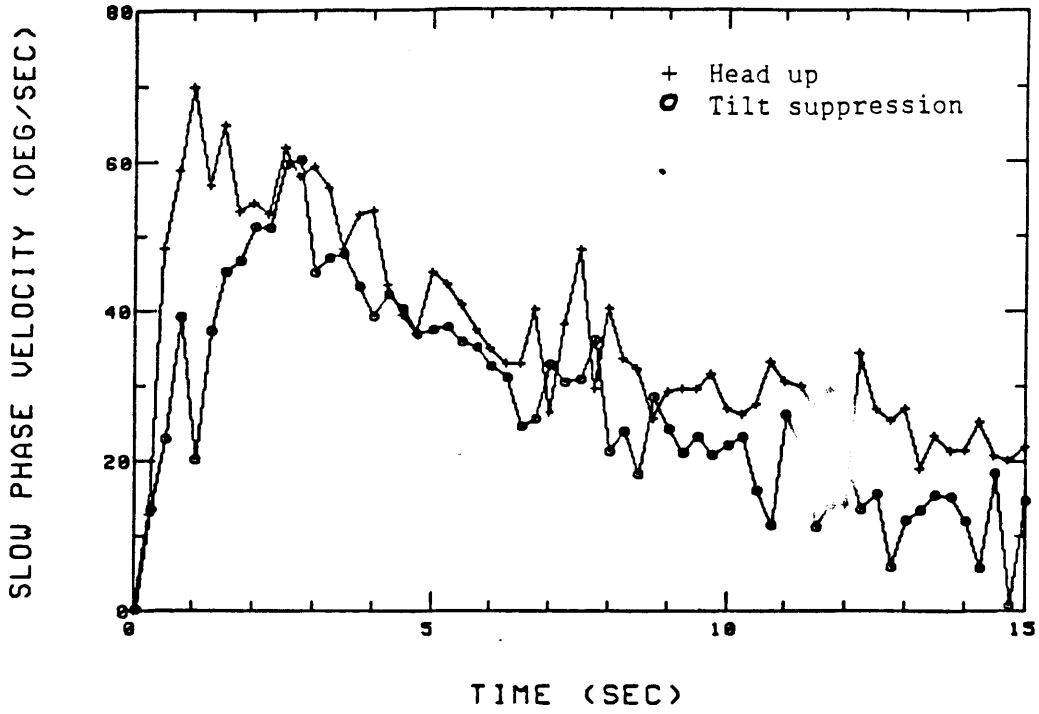

SUBJECT #2 POSTFLIGHT PVOR WITH/WITHOUT TILT SUPPRESSION

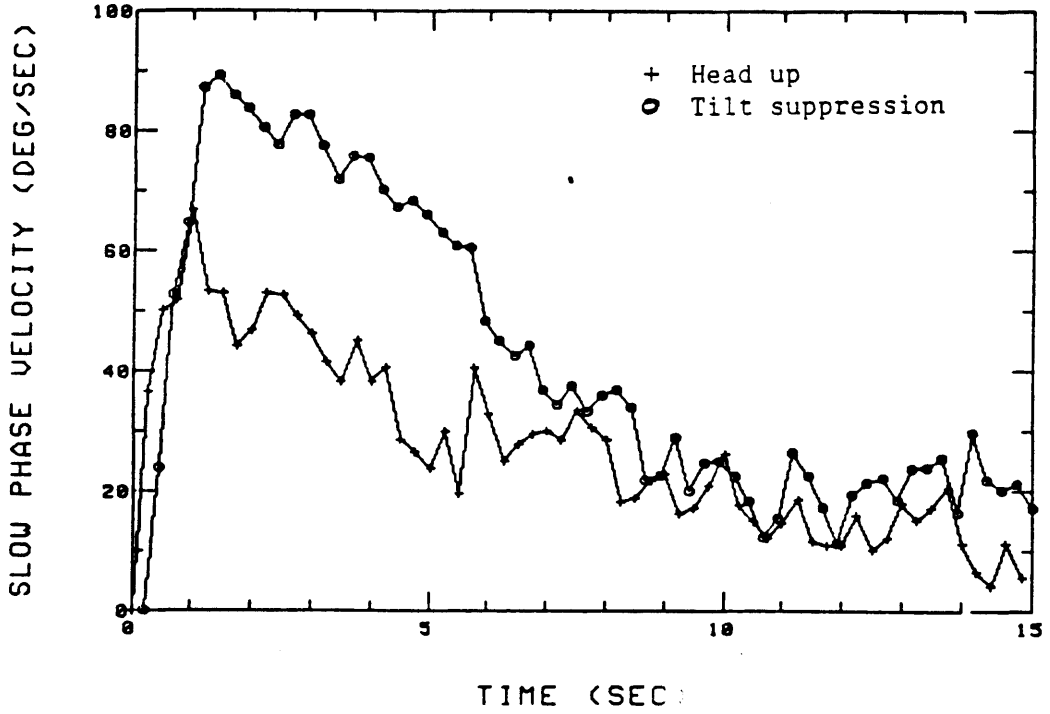

Fig. 7.1.4

SUBJECT #3 PREFLIGHT PVOR WITH/WITHOUT TILT SUPPRESSION

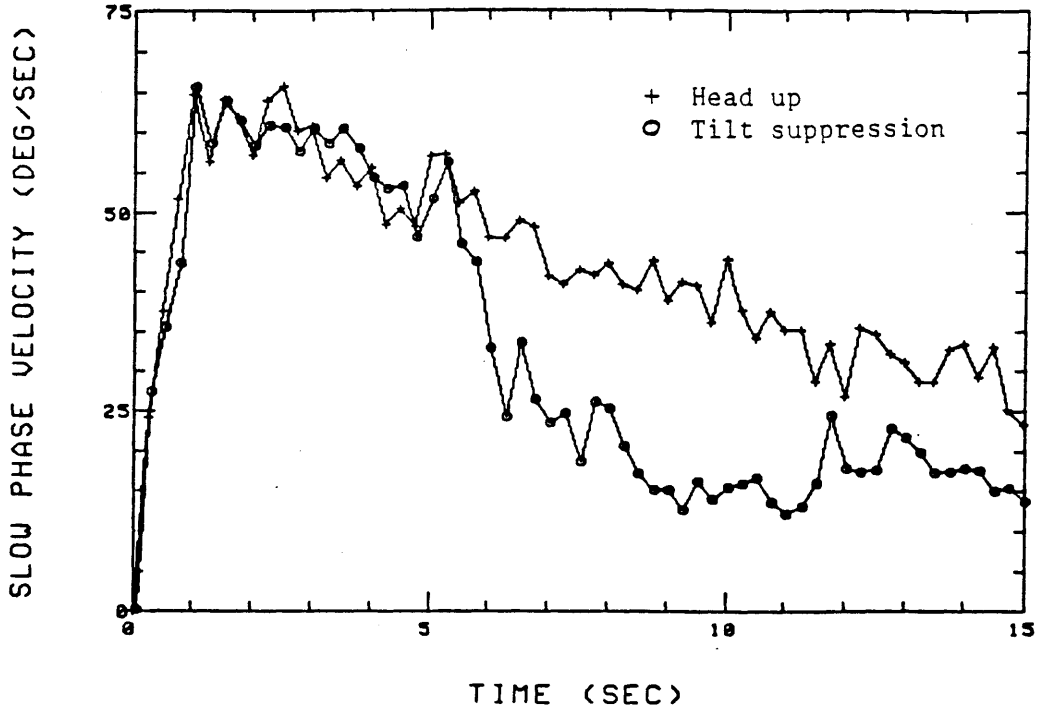

SUBJECT #3 POSTFLIGHT PVOR WITH/WITHOUT TILT SUPPRESSION

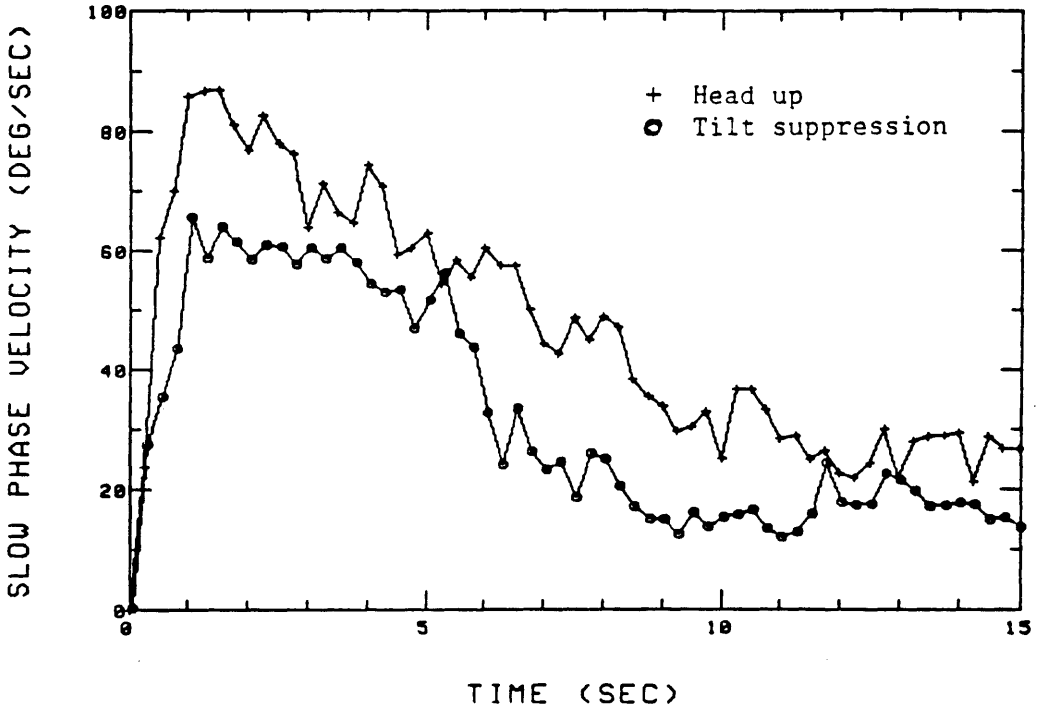

Fig. 7.1.5

SUBJECT #4 PREFLIGHT PVOR WITH/WITHOUT TILT SUPPRESSION

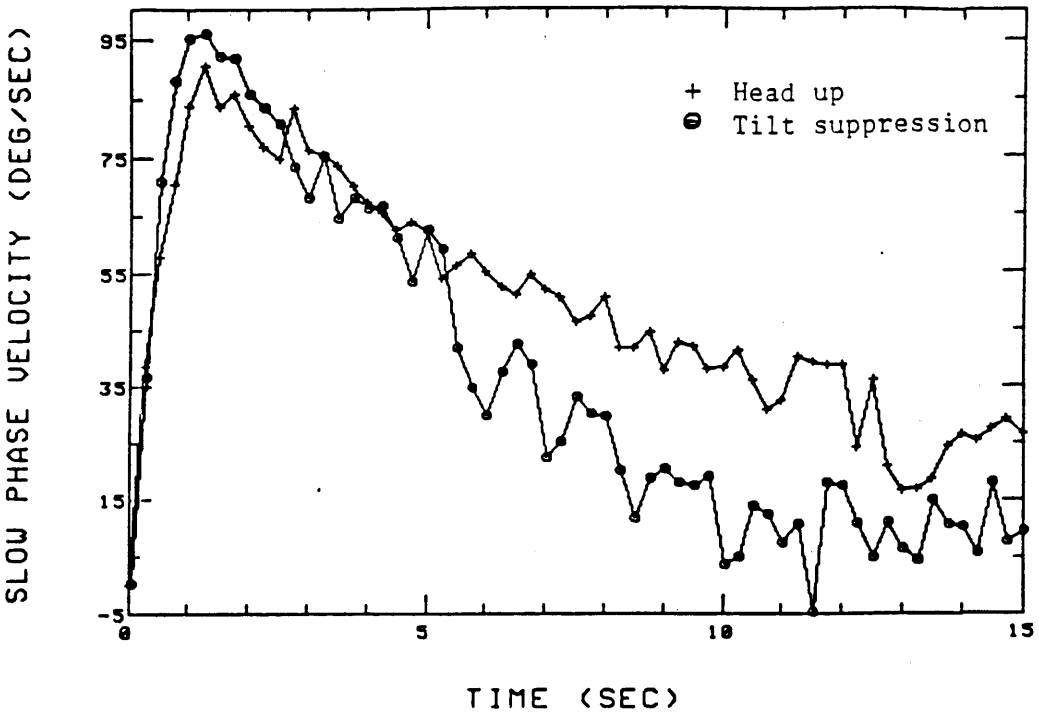

SUBJECT #4 POSTFLIGHT PVOR WITH/WITHOUT TILT SUPPRESSION

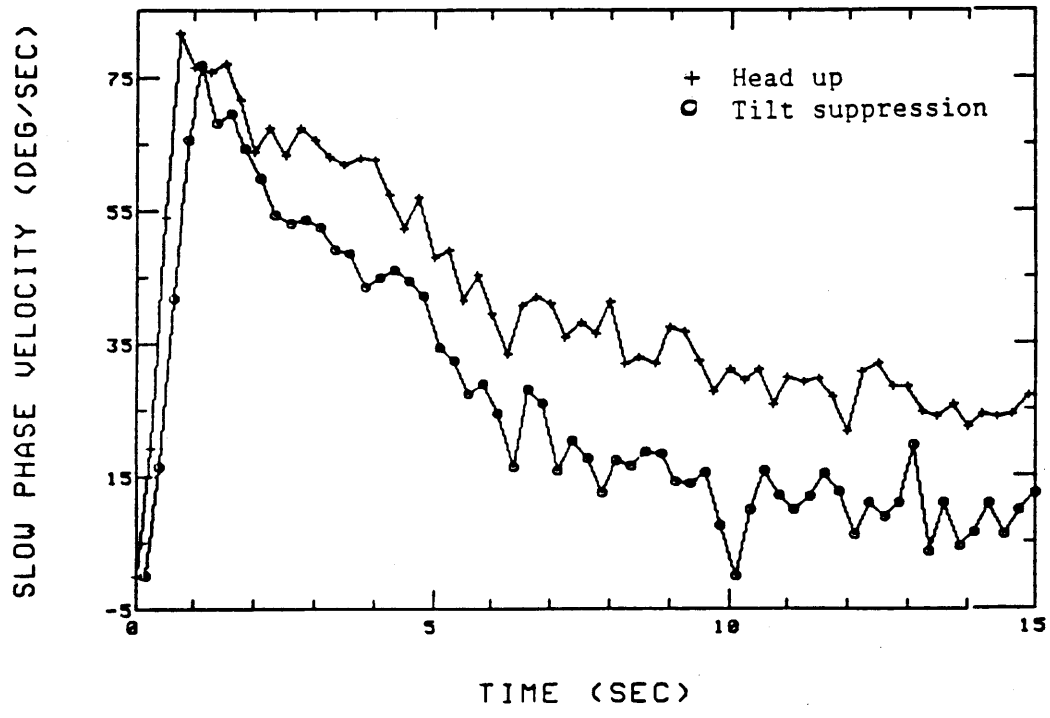

Fig 7.1.6

Chi-squared tests were performed on these plots to discover if individual subjects exhibited tilt suppression of nystagmus pre or postflight. In the tilt suppression tests, the head was tilted down from 5 to 10 seconds after the rotating chair stopped. Head up and head down responses from 5 to 10 seconds were compared with the chi-squared test. It indicated that preflight head up and tilt suppression responses from 5 to 10 seconds were significantly different with 95 % confidence for subjects 3 and 4. Postflight head up and tilt suppression responses from 5 to 10 seconds were significantly different for subject 2, 3, and 4, indicating that tilt suppression continued to occur postflight.

7.2 Mean Daily Responses of the Population

Regardless if the population preflight head up PVOR responses are calculated by averaging responses across subjects for each test day or by averaging across test days for each subject, the values of the means should be the same, though the variances and hence regression model fits could be different. Although each subjects PVOR response may vary greatly from each other, each subject may have consistent responses for each test day. It was hypothesized that the great variance in the responses between subjects made it hard to prove with a t-test analysis that the mean responses of the population were significantly different preflight and postflight. Thus another view of the mean preflight and postflight head up and tilt suppression responses was obtained by first averaging the responses of the 4 subjects on each of the five preflight testing days and each of the first two postflight testing days.

For each testing day, models were fit to the mean head up and head down responses averaged across the four subjects. Results of these model

fits are shown in Table 7.2.1.

DAYS PRELAUNCH OR POSTLANDING	HEAD UP TIME CONSTANT (SEC)	HEAD DOWN TIME CONSTANT (SEC)	GAIN
-151	11.0	3.5	.65
-121	12.7	3.5	.76
-65	19.6	2.5	.44
-43	11.0	4.1	.56
-10	12.2	2.2	.52
+1	9.1	2.3	.62
+2	9.5	4.4	.58
+4	12.3	3.5	.59

Daily model fits

Fig-7.2.1

Figure 7.2.2 shows in bar graph form the mean head up time constants for the population on each test day.

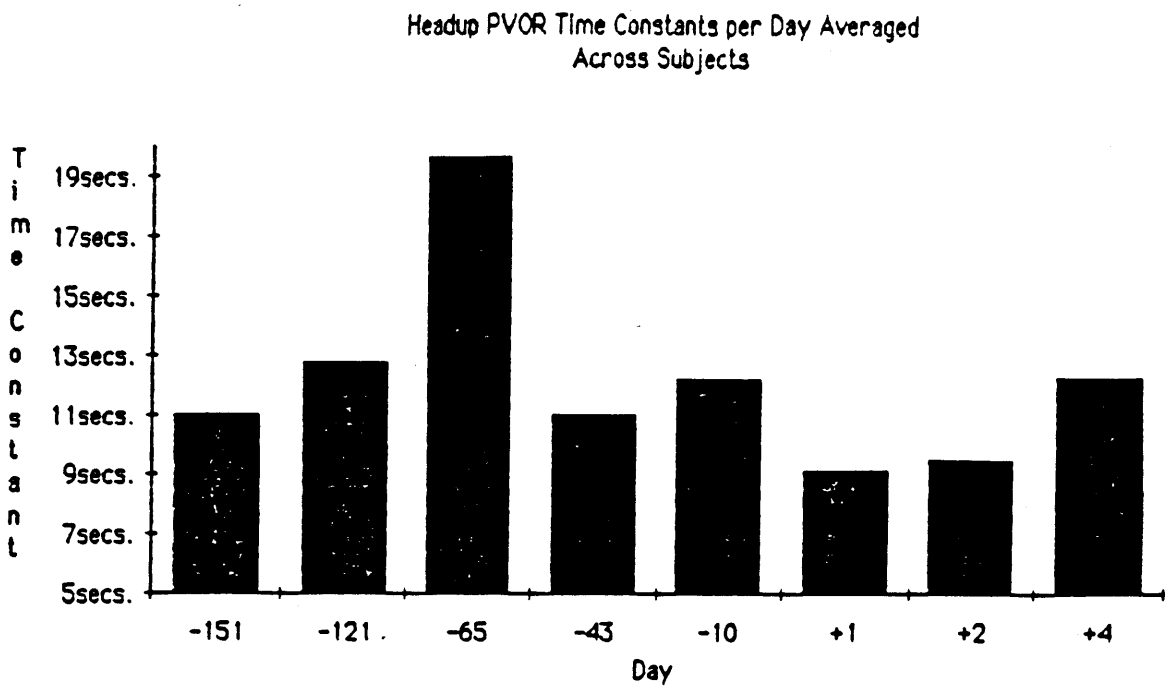

Fig 7.2.2 Results of model fits to preflight head up PVOR responses

Notice that the mean head up time constant of the population on the third test day (65 days prior to launch) is almost twice as large as the mean time constant of the population for the other two days. Although the variance of the daily mean preflight head up time constants is 13.0, the variance excluding the third test day is 0.9. This makes the accuracy of data from that day suspect, although no obvious explanation for the consistently longer responses could be found. Ignoring test day #3, the average of the daily mean preflight head up PVOR time constants +/- one standard deviation was 11.7 +/- 0.9 seconds. The postflight head up average for days +1 and +2 was 9.3 +/- 0.3 seconds. An independent

sample t-test indicated that the difference of the mean preflight and postflight head up PVOR responses was significant with 95% confidence.

The mean head down PVOR time constant on test day #3 did not look suspicious, although the head up time constant appeared different. The average of the five preflight daily mean head down time constants was 3.2 +/- 0.8 seconds. The mean postflight head down average for days +1 and +2 was 3.4 +/- 1.5 seconds. A t-test indicated that the difference in these means was not statistically significant.

7.3 GLobal Response of the Population

Up to now, we have averaged responses across days for each subject and have averaged responses across subjects for each day. Although the means are similar in each case, there is somewhat more variability between subjects than between days, especially if preflight day #3 is ignored. A third estimate of the mean response parameters of the population was obtained by averaging responses across days and across subjects. In other words, a mean response was calculated by averaging all tests of each subject on each day. Figure 7.3.1 shows mean preflight head up and tilt suppression responses from 0 to 15 seconds on the same plot.

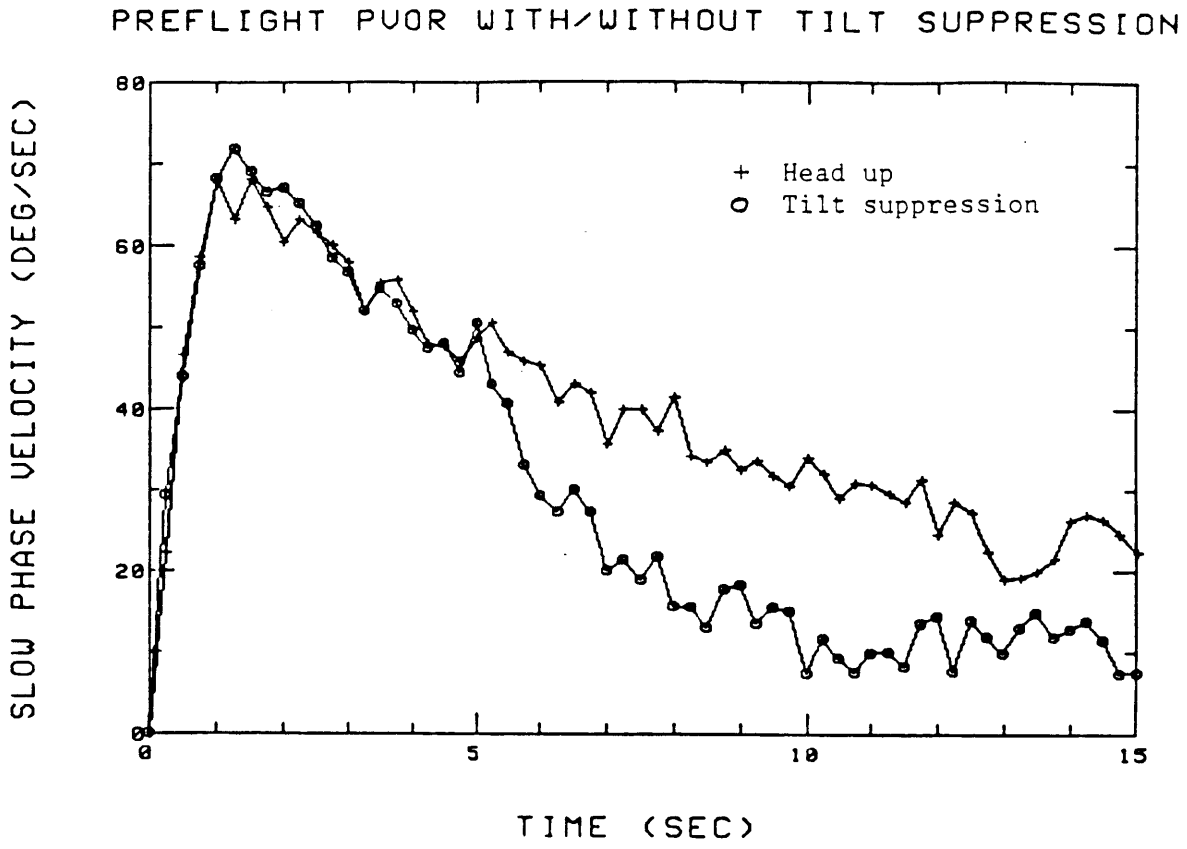

Fig. 7.3.1

The curves overlap from 0 to 5 seconds. However, slow phase velocity decayed more rapidly for the population when the head tilted forward at 5 seconds, consistent with Benson and Bodin's finding. When the head came upright at 10 seconds, the rate of decay decreased. Figure 7.3.2 shows the same data plotted on semi-ln axes.

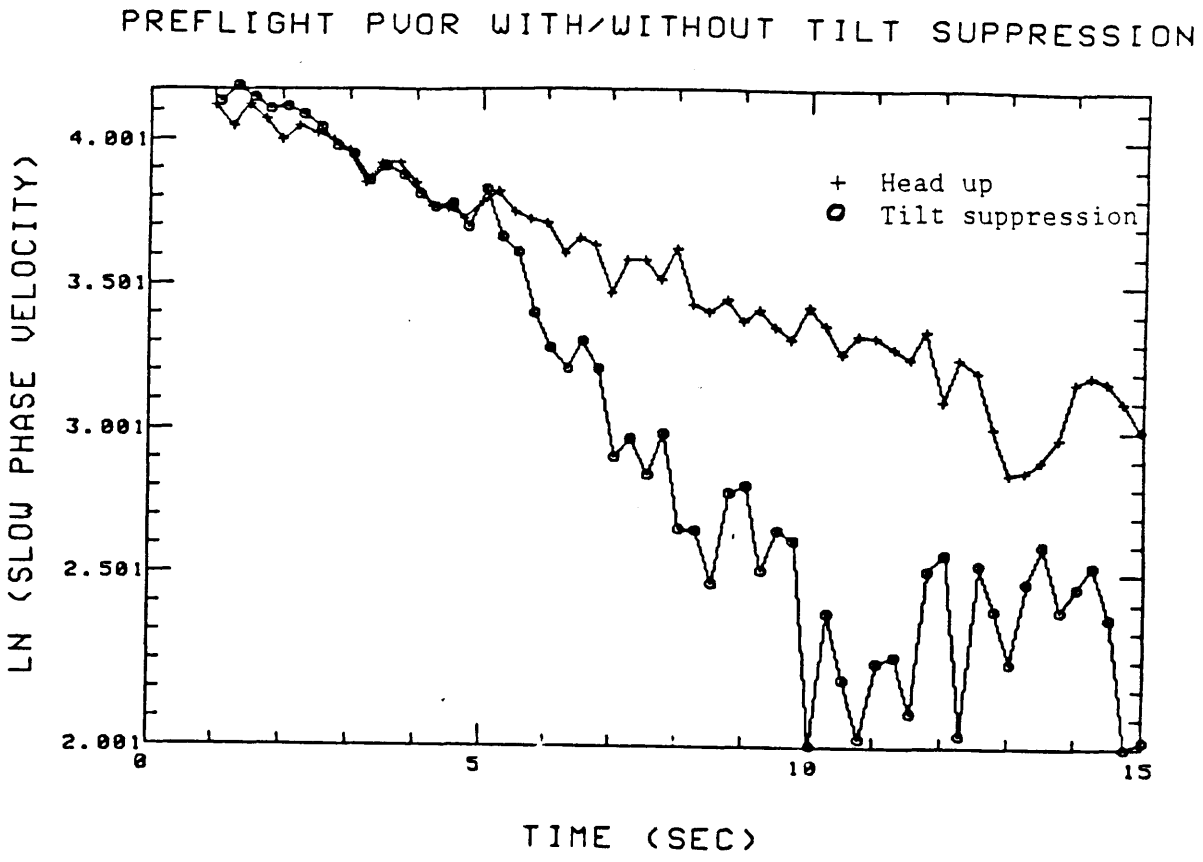

Fig. 7.3.2

Notice that the head up response appears to fit the one time constant model, at least for 20 seconds because the decay appears to be logarithmic, or linear when plotted on semi-ln axes. The rate of decay increases when the head tilts down. A chi-squared test indicated that the head up and tilt suppression responses were significantly different from 5 to 10 seconds.

Figure 7.3.3 shows the results of model fits for the preflight head up and tilt suppression responses. The time constant of the global preflight head up data was 12.8 seconds. The time constant of slow phase

velocity when the head was down from 5 to 10 seconds was 3.6 seconds. The global preflight gain was 0.59.

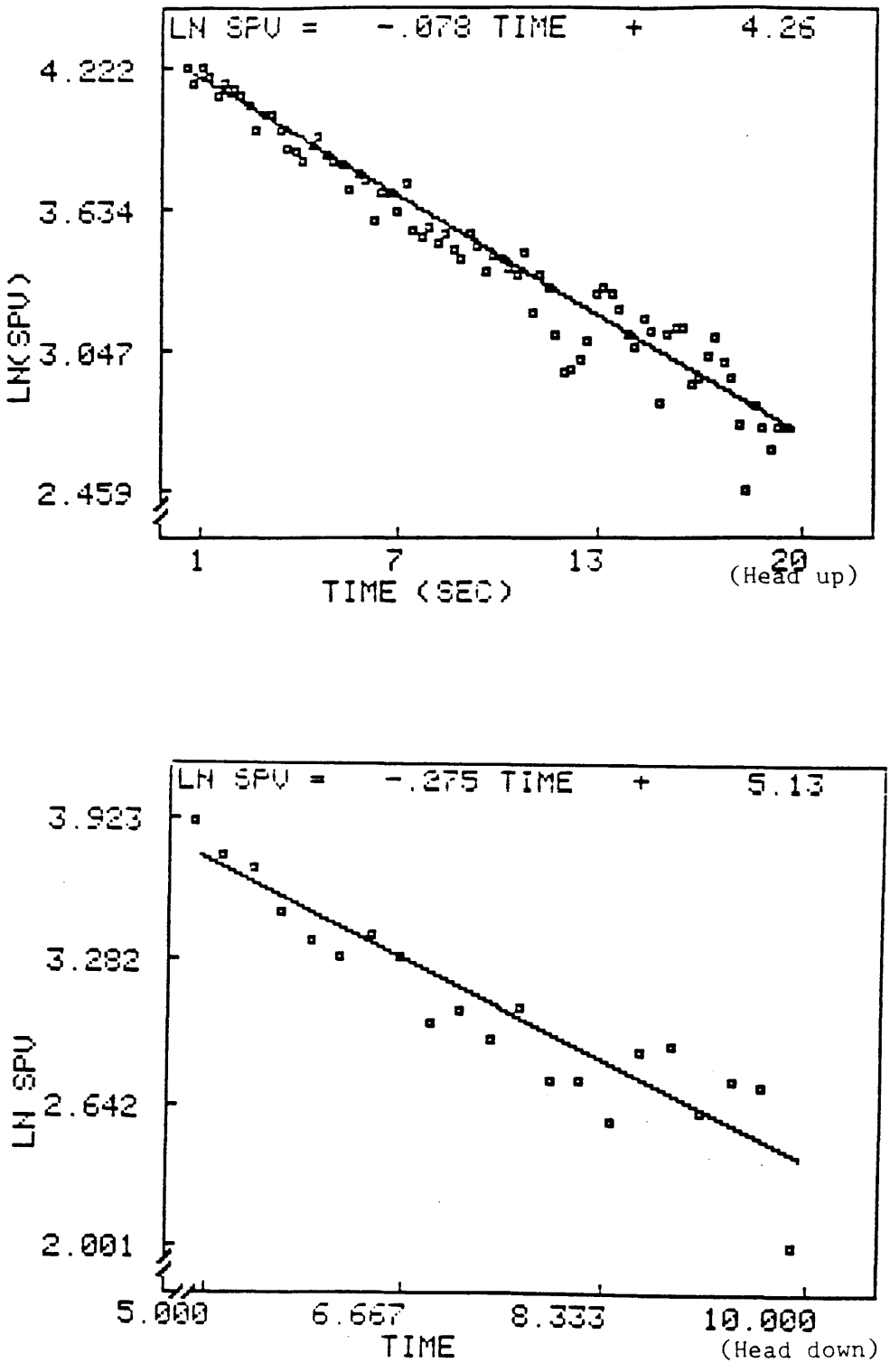

Fig. 7.3.3 Model fits for preflight PVOR tests

Fig. 7.3.3. Model fits of global preflight head up and tilt suppression tests.

Figure 7.3.4 shows the the mean postflight head up and tilt suppression responses obtained by averaging responses of the four subjects for the first two days of postflight testing.

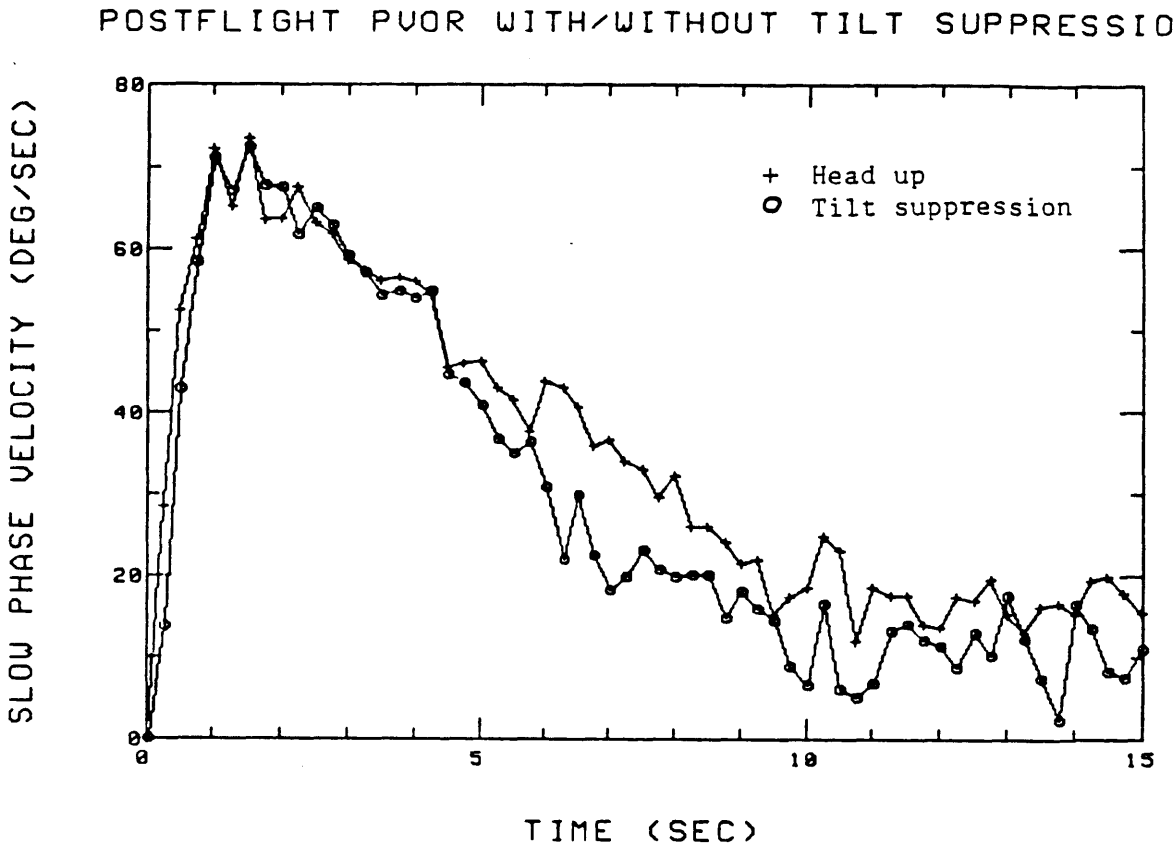

Fig 7.3.4

A chi-squared test on the head up and head down responses indicated that they were significantly different with 95% confidence. Notice that the tilt suppression does not appear as dramatic postflight as it did

preflight (Figure 7.3.2.). Model fits of the postflight head up and head down responses, which are shown in Figures 7.3.5 may explain this.

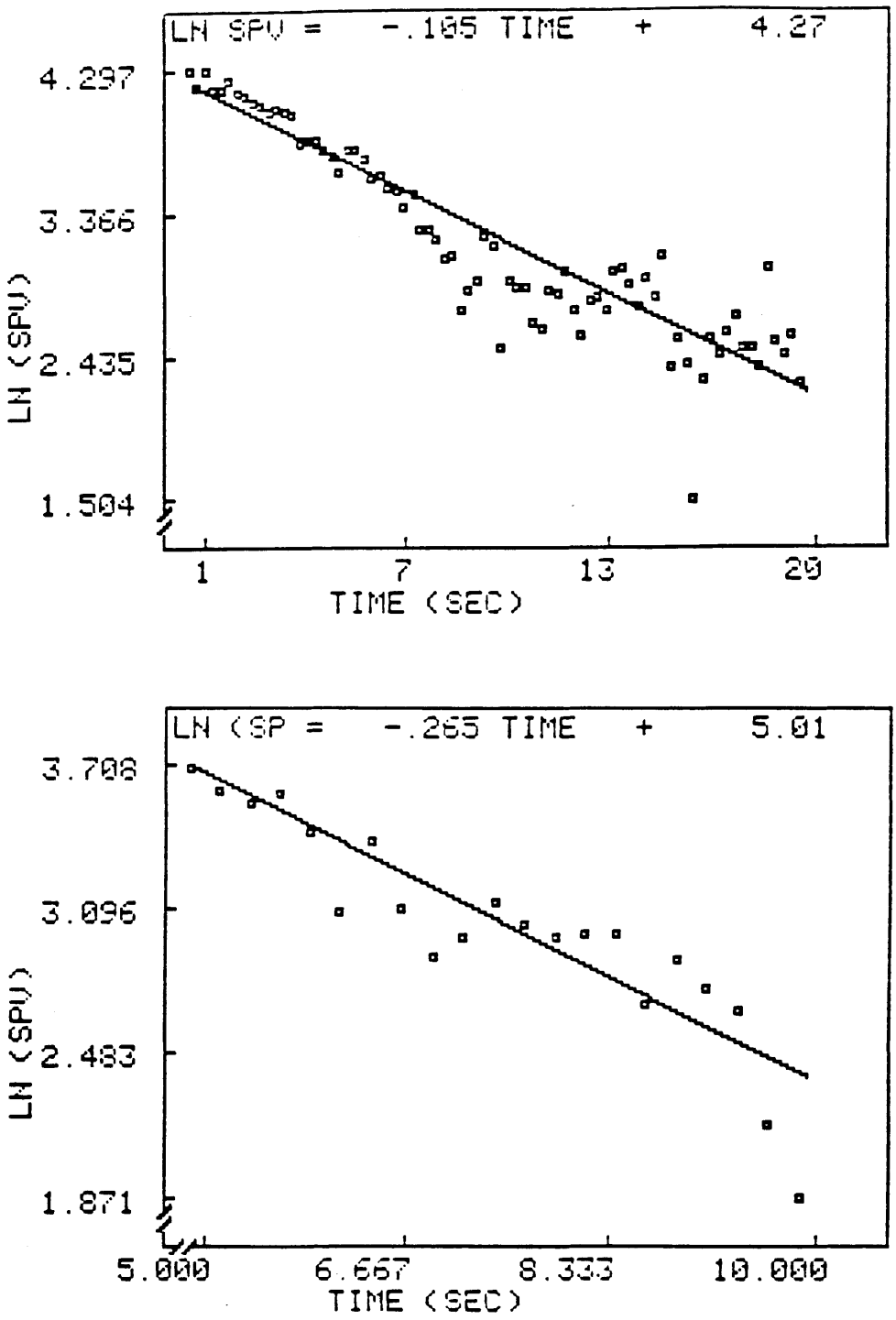

Fig 7.3.5. Model fits for postflight global head up and tilt suppression

The global postflight head up PVOR time constant was 9.5 seconds. The head down time constant was 3.8 seconds. The gain was 0.59. Thus the tilt suppression may appear more dramatic preflight than post flight for the global averaged responses because the postflight head up slow phase eye velocity decayed faster than the preflight head up velocity, which had an apparent time constant of 12.8 +/- seconds. By the time the head tilted forward post flight, the slow phase angular eye velocity had already decayed a good deal. The global model fits did not suggest that either the head down time constant or the gain changed preflight to post flight.

Figure 7.3.6 shows global pre and post flight head up PVOR responses in linear-linear and log-linear form. A chi-squared analysis of the global preflight vs postflight head up data showed no significant difference between 0 and 6 seconds, but a significant difference from 6 to 20 seconds (χ^2=111 for N=56). Since the first order model analysis did not show statistical significance unless data from test day three was omitted, it is not possible to conclusively interpret these findings.

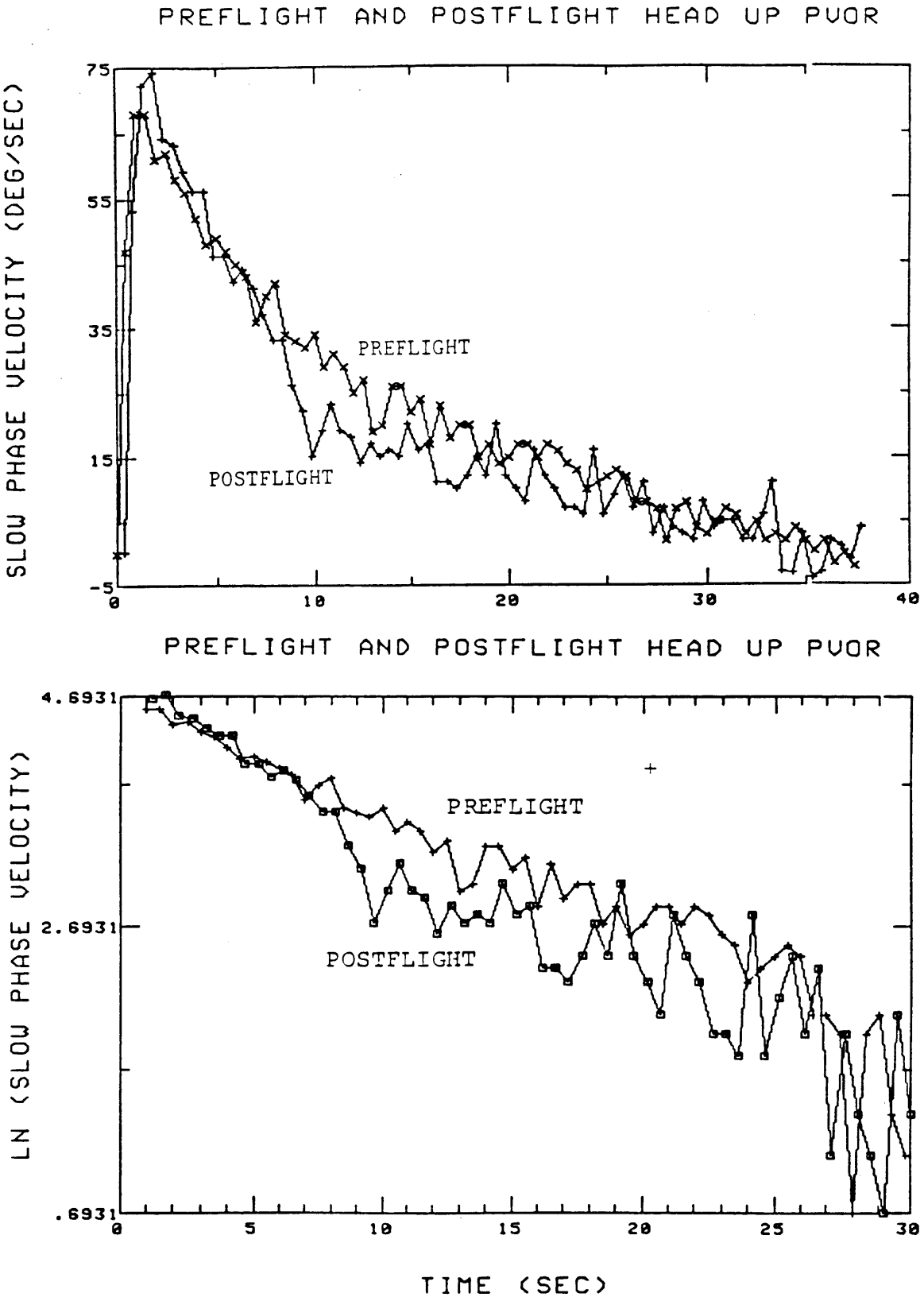

Fig. 7.3.6 Sample population pre and post flight head up responses.

Notice that the responses begin to diverge at about seven seconds.

However, Goldberg and Fernandez (1971) have shown that the time constant of afferent signals from the monkey semicircular canals is approximately 5 to 6 seconds. If human responses are similar, and PVOR is sustained by the Raphan/Cohen central velocity storage device, this analysis suggests that although weightlessness does not affect the dynamics of the semicircular canals, it makes the velocity storage integrator more leaky. Thus the pre and post flight head up PVOR responses are similar to 6 seconds, during the time epoch where eye velocity is driven mainly by the canals. After seven seconds, perhaps the afferent canal activity has largely decayed, and slow phase eye velocity is driven by the central integrator, which has become more leaky postflight.

Chapter 8

Discussion

There were five major conclusions from this investigation of the mean vestibulo-ocular responses of the sample population to a step angular head velocity.

1) The mean preflight head up PVOR profile was statistically significantly different between 5 and 10 seconds from the mean preflight head down profile for the sample population. Slow phase eye velocity was suppressed when the head tilted down. These finding confirm those of Benson and Bodin and others.

2) The mean postflight head up PVOR profile was statistically significantly different between 5 and 10 seconds from the mean postflight velocity profile for the first two days postflight for the sample population. Slow phase eye velocity was suppressed when the head tilted down.

3) Mean head up PVOR profiles were statistically significantly different preflight vs the first two days postflight during the period between 6 and 20 seconds after the chair stopped.

4) The preflight head down PVOR time constant was not statistically significantly different from than the mean postflight head down time constant for the sample population.

5) The preflight PVOR gain was not statistically significantly different from the postflight PVOR gain.

The evidence of preflight tilt suppression is consistent with a theory that the oculomotor system is driven partly by a gravity sensitive central velocity storage element. If the head tilts forward 90 degrees

when the afferent nerves from the horizontal semicircular canals are signaling rotation in their plane, the slow phase eye velocity falls more quickly than when the head remains upright. Thus the otolith organs might either open the pathway from the central velocity storage element to the oculomotor system, as shown in the bottom of Figure 2.5.1 or they might greatly increase the leak rate of the integrator element, as shown in the top of Figure 2.5.1. Afferent canal signals instead of afferent central integrator signals become the dominant stimulus to the oculomotor system when the head tilts.

If head tilt five seconds into a PVOR induced the otoliths to open the circuit between the velocity storage element and the oculomotor system, then slow phase eye velocity should instantaneously drop because eye movement would only be driven by the canals which have a very short time constant. The time constant of the slow phase velocity during head tilt would equal the physical time constant of the cupula-endolymph system, ignoring nonlinearities and adaptation affects. When the head was brought back upright, otoliths signals would complete the circuit between the central velocity storage element and the oculomotor system and eye velocity should instantaneously rise to the level it would have been at the time if the head was never tilted.

If head tilt five seconds into a PVOR induced the otoliths not to open the circuit between the velocity storage element and the oculomotor system, but to instead greatly increase the leak rate of the central integrator, different eye movement dynamics would be observed. Slow phase eye velocity would not instantaneously drop to the canal's estimate of head velocity. It would decrease with a much shorter time constant which was a function of the increased leak rate of the central

integrator.

The most powerful way to test which theory best models the physiological system is to observe slow phase eye velocity when the head is brought back upright during a PVOR tilt suppression test. If the otoliths open and close the circuit when the head tilts, eye velocity should instantaneously rise when the head is bought upright again and resume the head up decay profile. If instead the otoliths change the leak rate of the velocity integrator, eye velocity will remain at the same level when the head is brought upright because the integrator will have discharged during the tilt. However, both models predict the head up time constants before the head tilt and after the head is brought upright to be the same.

Signals recorded from individual subjects were too noisy to indicate conclusively if slow phase velocity rose when the head was brought up in a tilt suppression test. Subject 3 may have demonstrated that his preflight eye velocity increased after his head was brought upright in a tilt suppression test. However, it clearly did not climb up the level of the control head up response. This data was shown in Figure 7.1.5.

Because tilt suppression of nystagmus was observed both preflight and postflight and the preflight head down time constant was not significantly different from the postflight head down time constant, there was no evidence that the brain ignored signals from the otoliths after ten days in weightlessness. It is possible that any adaptation effects disappeared immediately after landing because the 1-g cues were overwhelmingly strong after spending ten days in weightlessness. If no tilt suppression occurred while in weightlessness, this would support

model which give the otoliths the ability to alter signal paths of the central velocity storage element as they used the gravity vector to signal measure head tilt.

An somewhat unexpected result of this investigation was to find that postflight head up PVOR response profile was significantly different from the preflight head up PVOR profile starting at seven seconds after the rotating chair was stopped. There is no evidence to indicate that weightlessness causes a change in the physical structure of the semicircular canals within a week. The shortened apparent time constant from 1 to 20 seconds, derived from a one time constant model fit, may be the result of an adaptation process within the central velocity storage element or even within higher level brain functions in which the brain learns to pay less attention, in general, to the vestibular system, and more attention to visual clues to drive the central velocity storage element.

Appendix I

Suggestions For Other Experiments

1) In the tilt suppression experiments of this investigation, the head was tilted forward five seconds after the chair was stopped and brought upright ten seconds after the rotating chair was stopped. By the time the head was brought upright, slow phase eye velocity had decreased to the level where the signal to noise ratio was a problem for analysis.. Thus it was difficult to observe how the slow phase velocity changed when the head was brought back upright. To test if the otoliths open the pathway from the central velocity integrator to the eyes or if the otoliths increase the leak rate of the central velocity integrator, the following protocol is suggested:

The per rotatory procedure is unchanged. However, the head should tilt forward one second after the chair stops and return upright five seconds after the chair stops. Assuming the canals can charge the central velocity integrator in one second, the slow phase velocity should be significantly greater than the noise level after only five seconds of post rotatory response regardless of whether the velocity climbs when the head returns upright. This protocol would also test the theory that the central velocity storage element does not contribute significantly to drive slow phase eye velocity until approximately seven seconds after the rotating chair stops.

2) The basis of the hypothesis that the preflight head down time constant would be different than the postflight head down time constant, after seven seconds from the stop of the rotating chair, was based on interesting results of other sensory adaptation experiments. It was suspected that the brain would learn to interpret differently signals

from the gravity sensing otoliths differently after a week in space. It is possible that after landing, the strong 1-g gravity cues immediately made the brain respect otolith signals again if it learned to ignore them in weightlessness. If tilt suppression tests were performed immediately after returning from orbit and they indicated that the postflight head down time constant was significantly different from the preflight head down time constant, this would be solid evidence of an adaptation process which occurred in space. However, if no significant difference between pre and post flight head down time constants was observed, then no conclusions could be made about adaptation because whether or not in space the brain learns to ignore signals from the otoliths which output their best estimate of the gravity vector, the strong 1-g cues immediately after returning to earth could quickly swamp evidence of a slow adaptation to weightlessness.

3) Further analysis of the existing Slacelab 1 data is possible. Second order Raphan-Cohen models should be fit to individual runs, and then a two way analysis of variance performed.

Appendix II

Listings of programs that resample, plot, and perform simple statistics on files of slow phase velocity

The following programs can be found in the directory DP0:[302,10] on the DEC RSX system in the Man-Vehicle Lab.

SR

This program resamples 38.4 seconds of a slow phase velocity signal from 100 Hz to 4 Hz so that it can be read by graphing and statistical programs. The program first asks for the name of the file to be resampled. This file must have 256 words per record. The program then asks if the sign of the velocity should be inverted. It outputs time and the resampled signal to a formatted sequential file with the same name as the input file except that the first letter has been replaced by an "S".

FRAPH

Fraph must be run on a graphics terminal. It plots a raw EOG signal and the corresponding 100 Hz slow phase velocity signal beneath it for 20 seconds. The program scales the EOG signal, but does not scale the velocity signal when plotting. Both position and velocity files must be sequential files. The position file must have extension (.EOG). THe velocity file must have extension (.SPV).

SRAPH

This program must be run on a graphics terminal. It plots a slow

phase velocity signal which has been sampled at 4 Hz vs time for 20 seconds. The program reads formatted sequential files in which the time and slow phase velocity is contained in each record.

PRO

This program finds the average, variance, standard deviation, and sample error of the mean of points in time from 0 to 37.75 seconds of sequential formatted slow phase eye velocity files sampled at 4 Hz. The program asks for the number of files to be averaged, and the name of the file to which it will write the formatted results sequentially. Each record in the output file contains the time, average, variance, standard deviation, standard error of the mean (sem), ave + (sem), and ave - (sem).

COMP

This program finds a chi-squared value relating the similarity of two mean velocity profiles sampled at 4 Hz using a pooled variance technique. The user inputs the names of the two files to be compared, the number of files averaged into each mean file, and the desired time interval for comparison. The program then outputs the number of points, N, which were compared and the corresponding chi-squared value. The user must then look up confidence intervals in chi-squared tables.

SEE

This program scrolls sequential files on the screen. It is designed specifically to type time or slow phase velocity from files that contain these parameters in the first to words of each record. There is a 6

second delay after the user hits return to execute the program. After all the data has scrolled, the user must hit the return key to exit the program.

```
        C ****** SR ******
        C THIS PROGRAM RESAMPLES A 38.4 SECOND DURATION
        C 100 HZ SIGNAL TO 4HZ AND CHANGES THE SIGN OF THE VALUES,
        C IF DESIRED

0001            REAL  Y(4000),RESAM(180),T
0002            CHARACTER*10 TEST,TEST2
0003            INTEGER BUF(256),S,C,J,K,L,ZERO,FLIP

        C READ IN FILE TO BE RESAMPLED

0004    2       TYPE*, ' ENTER FILE NAME'
0005            READ(5,3), TEST
0006    3       FORMAT(A10)
0007            TEST2=TEST
0008            TEST2(1:1)='S'
0009            TYPE*, ' FILE READ IS...', TEST
0010            TYPE*, ' FILE OPENED IS...', TEST2
0011    5       TYPE*, ' DO YOU WANT FILE INVERTED? (Y=1,N=0)'
0012            READ(5,7), FLIP
0013    7       FORMAT(I1)
0014    90      FORMAT(I1)
0015    95      FORMAT(F6.2,F6.1)
0016            TYPE*, FLIP
0017            IF(FLIP .EQ. 1)THEN
0018                S=-1
C               ELSEIF(FLIP .EQ. 0)THEN
C   J               S=1
0021            ELSE
0022                GOTO 5
0023            ENDIF
0024            CALL ASSIGN(1,TEST,10)
0025            DEFINE FILE 1(0,256,U,NREC)
0026            OPEN(UNIT=2, FILE=TEST2,FORM='FORMATTED',
              +       ACCESS='SEQUENTIAL',STATUS='NEW')
0027            C=0
0028            DO 10 J=1,15
0029                  READ(1'J)BUF
0030                  DO 20 K=1,256
0031                        C=C+1
0032                        Y(C)=BUF(K)*S
0033    20            CONTINUE
0034    10      CONTINUE
0035            CLOSE(1)

        C RESAMPLE FILE TO 4 HZ

0036            C=0
0037            ZERO=0
0038            DO 15 M=1,152
0039                  WRITE(2,90), ZERO
0040    15      CONTINUE
C               CLOSE(2)
0042            Y(1)=0.0
0043            OPEN(UNIT=2,NAME=TEST2,FORM='FORMATTED',ACCESS='SEQUENTIAL'
              +       ,STATUS='OLD')
```

```
0                DO 30 L=1,3800,25
(   )                  C=C+1
0046                   T=L/100.-.01
0047                   RESAM(C)=Y(L)
0048                   WRITE(2,95) T,RESAM(C)
0049     30        CONTINUE
0050               CLOSE(2)
0051               CLOSE(1)
0052               GOTO 2
0053               END
```

P' 'RAM SECTIONS

Number	Name	Size		Attributes
1	$CODE1	001214	326	RW,I,CON,LCL
2	$PDATA	000304	98	RW,D,CON,LCL
3	$IDATA	000010	4	RW,D,CON,LCL
4	$VARS	041572	8637	RW,D,CON,LCL

VARIABLES

Name	Type	Address	Name	Type	Address	Name	Type	Address	Name
C	I*2	4-041552	FLIP	I*2	4-041564	J	I*2	4-041554	K
M	I*2	4-041570	NREC	I*2	4-041566	S	I*2	4-041550	T
TEST2	CHR	4-040536	ZERO	I*2	4-041562				

ARRAYS

Name	Type	Address	Size		Dimensions
BUF	I*2	4-040550	001000	256	(256)
RESAM	R*4	4-037200	001320	360	(180)
Y	R*4	4-000000	037200	8000	(4000)

LABELS

Label	Address	Label	Address	Label	Address	Label	Address	Label	Add
2	1-000020	3'	2-000000	5	1-000256	7'			
15	**	20	**	30	**	90'			

FUNCTIONS AND SUBROUTINES REFERENCED

ASSIGN CLOS$ OPEN$

Total Space Allocated = 043322 9065

```
      C ****** FRAPH ******
      C THIS PROGRAM USES THE VERSAPLOT SUBROUTINES TO GRAPH
      C A RAW EOG SIGNAL AND A SLOW PHASE  EYE VELOCITY SIGNAL
      C VS TIME.  THE VELOCITY SIGNAL WAS FORMATTED BY THE PROGRAM
      C "BRENDA"

0001            PROGRAM EOG5PT
0002            REAL X(2100), Y(2100),YSCALE(4)
0003            LOGICAL*1 FILE(6),FILE1(10),FILE2(10)
0004            INTEGER YTEMP(256),POINTS,YMAX,YMIN
0005            WRITE(5,2)
0006    2       FORMAT(' ENTER FILENAME...')
0007            READ(5,3)FILE
0008    3       FORMAT(6A1)
0009            FACT=1.2
0010            DO 7 L=1,6
0011                    FILE1(L)=FILE(L)
0012                    FILE2(L)=FILE(L)
0013    7       CONTINUE
0014            FILE1(7)='.'
0015            FILE2(7)='.'
0016            FILE1(8)='E'
0017            FILE2(8)='S'
0018            FILE1(9)='O'
0019            FILE2(9)='P'
(   )           FILE1(10)='G'
(   )           FILE2(10)='V'
0022            YMAX=0
0023            YMIN=0
0024            CALL ASSIGN(2,FILE2,10)
0025            DEFINE FILE 2(0,256,U,NREC)
0026            DO 8 L=1,8
0027                    READ(2'L)YTEMP
0028                    DO 9 M=1,256
0029                            IF(YTEMP(M).GT.YMAX)THEN
0030                                    YMAX=YTEMP(M)
0031                            ELSEIF(YTEMP(M).LT.YMIN)THEN
0032                                    YMIN=YTEMP(M)
0033                            ENDIF
0034    9                       CONTINUE
0035    8       CONTINUE
0036            CALL CLOSE(2)
0037            YSCALE(1)=YMAX/4096.
0038            YSCALE(2)=YMIN/4096.
0039            CALL ASSIGN(2,FILE2,10)
0040            DEFINE FILE 2(0,256,U,NREC)
0041            DO 10 J=0,2047
0042                    X(J+1)=J/100.
0043    10      CONTINUE
0044            J=0
0045            DO 20 K=1,8
(   )                   READ(2'K)YTEMP
(   )                   DO 30 I=1,256
0048                    J=J+1
0049                    Y(J)=YTEMP(I)/1.0
0050    30              CONTINUE
```

```
0       20      CONTINUE
0052            POINTS=2000
0053            CALL AERASE
0054            CALL PLOTS(0,0,1)
0055            CALL FACTOR(FACT)
0056            CALL PLOT(1.0,1.0,-3)
0057            CALL SCALE(YSCALE,6.,2,1)
0058            X(POINTS+1)=0.0
0059            X(POINTS+2)=2.0
0060            Y(POINTS+1)=-150.0
0061            Y(POINTS+2)=50.0
0062            CALL AXIS(0.,0.,9HTIME[SEC],-9,10.0,0.,X(POINTS+1),X(POINTS+2))
0063            CALL AXIS(0.,0.,3HSPV,+3,6.,90.,Y(POINTS+1),Y(POINTS+2))
0064            CALL LINE(X,Y,POINTS,1,0,1)
0065            CALL SYMBOL(6.,5.,0.5,FILE,0.,6)

        C
        C       DO 60 J=1024,2047
        C               X(J-1023)=J/100.
        C60     CONTINUE
        C       J=0
        C       DO 70 K=5,8
        C               READ(2'K)YTEMP
        C               DO 80 I=1,256
        C               J=J+1
        C               Y(J)=YTEMP(I)/4096.
        C80             CONTINUE
        C70     CONTINUE
        C       CALL LINE(X,Y,POINTS,1,0,1)
        C
        C
        C
0066            J=0
0067            DO 100 J=0,2047
0068                    X(J+1)=J/100.
0069    100     CONTINUE
0070            POINTS=2000
0071            X(POINTS+1)=0.0
0072            X(POINTS+2)=2.0
0073            CALL ASSIGN(1,FILE1,10)
0074            DEFINE FILE 1(0,256,U,NREC)
0075            J=0
0076            DO 120 K=1,8
0077                    READ(1'K)YTEMP
0078                    DO 130 I=1,256
0079                    J=J+1
0080                    Y(J)=YTEMP(I)/4096.
0081    130             CONTINUE
0082    120     CONTINUE
0083            CALL PLOT(0.,6.50,-3)
0084            CALL SCALE(Y,1.,POINTS,1)
0085            CALL AXIS(0.,0.,9HTIME[SEC],-9,10.0,0.,X(POINTS+1),X(POINTS+2))
0086            CALL AXIS(0.,0.,3HEOG,+3,1.,90.,Y(POINTS+1),Y(POINTS+2))
0087            CALL LINE(X,Y,POINTS,1,0,1)
        C       DO 150 L=1024,2047
        C               X(L-1023)=L/100.
```

```
C150    CONTINUE
C       J=0
C       DO 200 K=5,8
C               READ(1'K)YTEMP
C               DO 250 I=1,256
C                       J=J+1
C                       Y(J)=YTEMP(I)/4096.
C250            CONTINUE
C200    CONTINUE
C       CALL LINE(X,Y,POINTS,1,0,1)
C       CALL PLOT(0.,0.,+999)
C       READ(5,*)
C       CALL GERASE
C       DO 1000 J=2000,2999
C               X(J-1999)=J/100.
C1000   CONTINUE
C       J=0
C       DO 2000 K=9,12
C               READ(2'K)YTEMP
C               DO 3000 I=1,250
C               J=J+1
C               Y(J)=YTEMP(I)/4096.
C3000           CONTINUE
C2000   CONTINUE
C       CALL AERASE
C       X(POINTS+1)=20.0
C       Y(POINTS+1)=YSCALE(3)
C       Y(POINTS+2)=YSCALE(4)
C       CALL PLOTS(0,0,1)
C       CALL FACTOR(FACT)
C       CALL PLOT(1.0,1.0,-3)
C       CALL AXIS(0.,0.,9HTIME[SEC],-9,10.0,0.,X(POINTS+1),X(POINTS+2))
C       CALL AXIS(0.,0.,3HEOG,+3,6.0,90.,Y(POINTS+1),Y(POINTS+2))
C       CALL LINE(X,Y,POINTS,1,0,1)
C
C       DO 6000 J=3000,3999
C               X(J-2999)=J/100.
C6000   CONTINUE
C       J=0
C       DO 7000 K=13,16
C               READ(2'K)YTEMP
C               DO 8000 I=1,250
C               J=J+1
C               Y(J)=YTEMP(I)/4096.
C8000           CONTINUE
C7000   CONTINUE
C       CALL LINE(X,Y,POINTS,1,0,1)
C
C
C
C       DO 10000 J=2000,2999
C               X(J-1999)=J/100.
C10000  CONTINUE
C       J=0
C       DO 12000 K=9,12
C               READ(1'K)YTEMP
```

```
C                DO 13000 I=1,250
C                J=J+1
C                Y(J)=YTEMP(I)/4096.
C13000           CONTINUE
C12000   CONTINUE
C        CALL PLOT(0.,6.5,-3)
C        CALL SCALE(Y,1.,POINTS,1)
C        CALL AXIS(0.,0.,9HTIME[SEC],-9,10.0,0.,X(POINTS+1),X(POINTS+2))
C        CALL AXIS(0.,0.,8HVELOCITY,+8,1.,90.,Y(POINTS+1),Y(POINTS+2))
C        CALL LINE(X,Y,POINTS,1,0,1)
C        DO 15000 L=3000,3999
C                X(L-2999)=L/100.
C15000   CONTINUE
C        J=0
C        DO 20000 K=13,16
C                READ(1'K)YTEMP
C                DO 25000 I=1,250
C                        J=J+1
C                        Y(J)=YTEMP(I)/4096.
C25000           CONTINUE
C20000   CONTINUE
C        CALL LINE(X,Y,POINTS,1,0,1)
0088             CALL CLOSE(1)
0089             CALL CLOSE(2)
C        CALL PLOT(0.,0.,+999)
C        READ(5,*)
C        CALL GERASE
0090             STOP
0091             END
```

F RAM SECTIONS

Number	Name	Size		Attributes
1	$CODE1	001746	499	RW,I,CON,LCL
2	$PDATA	000326	107	RW,D,CON,LCL
3	$IDATA	000106	35	RW,D,CON,LCL
4	$VARS	041740	8688	RW,D,CON,LCL
5	$TEMPS	000002	1	RW,D,CON,LCL

VARIABLES

Name	Type	Address	Name	Type	Address	Name	Type	Address	Name
FACT	R*4	4-041720	I	I*2	4-041736	J	I*2	4-041732	K
M	I*2	4-041730	NREC	I*2	4-041726	POINTS	I*2	4-041712	YMAX

ARRAYS

Name	Type	Address	Size		Dimensions
FILE	L*1	4-040660	000006	3	(6)
FILE1	L*1	4-040666	000012	5	(10)
E2	L*1	4-040700	000012	5	(10)
	R*4	4-000000	020320	4200	(2100)
Y	R*4	4-020320	020320	4200	(2100)
YSCALE	R*4	4-040640	000020	8	(4)
YTEMP	I*2	4-040712	001000	256	(256)

LABELS

Label	Address	Label	Address	Label	Address	Label	Address	Label	Add
2'	2-000000		3'	2-000026		7	**	8	
10	**		20	**		30	**	100	
130	**								

FUNCTIONS AND SUBROUTINES REFERENCED

AERASE ASSIGN AXIS CLOSE FACTOR LINE PLOT PLOTS SCALE SYMBOL

Total Space Allocated = 044344 9330

```
      C ****** SRAPH ******
      C THIS PROGRAM USES THE VERSAPLOT SUBROUTINES
      C TO GRAPH SIGNALS IN TIME.  IT ONLY READS
      C FILES WHICH WERE FORMATTED BY THE PROGRAMS "SR"
      C OR "PRO'

0001            PROGRAM EOG5PT
0002            REAL X(2050), Y(2050),YSCALE(4),SAMP
0003            LOGICAL*1 FILE(10)
0004            INTEGER YTEMP(256),POINTS,YMAX,YMIN
0005            WRITE(5,2)
0006    2       FORMAT(' ENTER FILENAME...')
0007            READ(5,3)FILE
0008    3       FORMAT(10A1)
0009            FACT=1.2
0010    9       FORMAT(F6.2,F6.1)
0011            OPEN(UNIT=2,NAME=FILE,FORM='FORMATTED',
              +      ACCESS='SEQUENTIAL',STATUS='OLD')
0012            DO 15 J=1,80
0013                  READ(2,9), TM,SAMP
0014                  C=C+1
0015                  Y(C)=SAMP
0016    15      CONTINUE
0017            C=0
0018            DO 18 K=1,80
0                     C=C+1
0                     X(C)=K/4.0
0021    18      CONTINUE

0022            POINTS=78
0023            CALL AERASE
0024            CALL PLOTS(0,0,1)
0025            CALL FACTOR(FACT)
0026            CALL PLOT(1.0,1.0,-3)
0027            CALL SCALE(YSCALE,6.,2,1)
0028            X(POINTS+1)=0.0
0029            X(POINTS+2)=2.0
0030            Y(POINTS+1)=-150.0
0031            Y(POINTS+2)=50.0
0032            CALL AXIS(0.,0.,9HTIME[SEC],-9,10.0,0.,X(POINTS+1),X(POINTS+2))
0033            CALL AXIS(0.,0.,3HSPV,+3,6.,90.,Y(POINTS+1),Y(POINTS+2))
0034            CALL LINE(X,Y,POINTS,1,0,1)
0035            CALL SYMBOL(6.,5.,0.5,FILE,0.,6)
0036            CLOSE (2)
0037            END
```

PROGRAM SECTIONS

Number	Name	Size		Attributes
1	$CODE1	000600	192	RW,I,CON,LCL
2	$PDATA	000310	100	RW,D,CON,LCL
3	$IDATA	000054	22	RW,D,CON,LCL
4	$VARS	041104	8482	RW,D,CON,LCL
5	$TEMPS	000002	1	RW,D,CON,LCL

VARIABLES

Name	Type	Address	Name	Type	Address	Name	Type	Address	Name
C	R*4	4-041076	FACT	R*4	4-041064	J	I*2	4-041070	K
SAMP	R*4	4-040040	TM	R*4	4-041072	YMAX	I*2	4-041060	YMIN

ARRAYS

Name	Type	Address	Size		Dimensions
FILE	L*1	4-040044	000012	5	(10)
X	R*4	4-000000	020010	4100	(2050)
	R*4	4-020010	020010	4100	(2050)
SCALE	R*4	4-040020	000020	8	(4)
YTEMP	I*2	4-040056	001000	256	(256)

LABELS

Label	Address	Label	Address	Label	Address	Label	Address	Label	Add
2'	2-000000	3'	2-000026	9'	2-000032	15			

FUNCTIONS AND SUBROUTINES REFERENCED

AERASE AXIS CLOS$ FACTOR LINE OPEN$ PLOT PLOTS SCALE SYMBOL

Total Space Allocated = 042272 8797

```
      C ****** PRO ******
      C THIS PROGRAM FINDS THE AVERAGE, STANDARD DEVIATION
      C AND SAMPLE ERROR OF THE MEAN OF POINTS IN TIME FROM 0 TO
      C 37.75 SECONDS OF SEQUENTIAL FORMATTED FILES SAMPLED AT 4 HZ.

0001          INTEGER C,N,P,J,K,L
0002          REAL BUF(152),SUM(152),SQU(152),SEM1(152),SEM2(152),TM
0003          REAL AVE(152),DIF(152),VAR(152),SDV(152),SEM(152),T(152)
0004          CHARACTER*10 SEQ(58)
0005          CHARACTER*10 OUT
0006          TYPE*, ' ENTER NUMBER OF FILES TO BE AVERAGED'
0007          READ(5,10), N
0008    10    FORMAT(I2)
0009    20    FORMAT(A10)
0010    25    FORMAT(F6.2,F6.1)

      C       READ IN FILE NAMES

0011          DO 30 J=1,N
0012              TYPE*, J
0013              TYPE*, ' ENTER FILE NAME'
0014              READ(5,20), SEQ(J)
0015    30    CONTINUE
0016          TYPE*, ' THE FOLLOWING FILES WILL BE AVERAGED'
0017          DO 40 K=1,N
0018                TYPE*, SEQ(K)
0019    40    CONTINUE
0020          C=0
0021          TYPE*, ' ENTER THE NAME OF THE OUTPUT FILE'
0022          READ(5,20), OUT

      C FIND THE AVERAGE FOR EACH POINT

0023    45    C=C+1
0024          TYPE*, ' FILE ABOUT TO BE READ IS...',C
0025          OPEN(UNIT=1,NAME=SEQ(C),ACCESS='SEQUENTIAL',
             +     FORM='FORMATTED',STATUS='OLD')
0026          DO 50 L=1,152
0027             READ(1,25), TM,BUF(L)
0028             SUM(L)=SUM(L)+BUF(L)
0029    50    CONTINUE
0030          CLOSE(1)
0031          IF(C .LT. N)THEN
0032             GOTO 45
0033          ENDIF
0034          DO 60 L=1,152
0035             AVE(L)=SUM(L)/N
0036    60    CONTINUE
0037          C=0
0038          TYPE*, N,' FILES AVERAGED'

      C   FIND THE SUM OF SQUARES FOR EACH POINT

0039    65    C=C+1
0040          OPEN(UNIT=1,NAME=SEQ(C),ACCESS='SEQUENTIAL',STATUS='OLD')
0041          DO 70 L=1,152
```

```
0                READ(1,25), TM,BUF(L)
0043             DIF(L)=BUF(L)-AVE(L)
0044             SQU(L)=SQU(L)+DIF(L)*DIF(L)
0045     70      CONTINUE
0046             CLOSE(1)
0047             IF(C .LT. N)THEN
0048                GOTO 65
0049             ENDIF
0050             C=0
0051             TYPE*, ' SUM OF SQUARES CALCULATED'

         C FIND THE VARIANCE AND STD DEV FOR EACH POINT

0052             DO 75 J=1,152
0053                   VAR(J)=(SQU(J)/(N-1))
0054                   SDV(J)=(VAR(J))**0.5
0055     75      CONTINUE
0056             TYPE*, ' VARIACE CALCULATED'
0057             TYPE*, ' SDV CALCULATED'

         C FIND THE STANDARD ERROR OF THE MEAN FOR EACH POINT

0058             DO 90 L=1,152
0059                SEM(L)=SDV(L)/(N**0.5)
0060                SEM1(L)=AVE(L)+SEM(L)
0                   SEM2(L)=AVE(L)-SEM(L)
0        90      CONTINUE
0003             TYPE*, ' SEM CALCULATED'

         C WRITE THE RESULTS TO A FILE

0064             OPEN(UNIT=2,NAME=OUT,FORM='FORMATTED',ACCESS='SEQUENTIAL',
                +      STATUS='NEW')
0065             DO 95 P=1,152
0066                T(P)=P/4.0-.25
0067                WRITE(2,100), T(P),AVE(P),VAR(P),SDV(P),SEM(P),SEM1(P),SEM2(P
0068     95      CONTINUE
0069     100     FORMAT(F6.2,F6.1,F8.1,4F6.1)
0070             END
```

RAM SECTIONS

Number	Name	Size		Attributes
1	$CODE1	002202	577	RW,I,CON,LCL
2	$PDATA	000464	154	RW,D,CON,LCL
3	$IDATA	000060	24	RW,D,CON,LCL
4	$VARS	016176	3647	RW,D,CON,LCL
5	$TEMPS	000006	3	RW,D,CON,LCL

VARIABLES

Name	Type	Address	Name	Type	Address	Name	Type	Address	Name
C	I*2	4-000000	J	I*2	4-000006	K	I*2	4-000010	L
OUT	CHR	4-016164	P	I*2	4-000004	TM	R*4	4-005754	

ARRAYS

Name	Type	Address	Size		Dimensions
AVE	R*4	4-005760	001140	304	(152)
BUF	R*4	4-000014	001140	304	(152)
	R*4	4-007120	001140	304	(152)
	R*4	4-011420	001140	304	(152)
SEM	R*4	4-012560	001140	304	(152)
SEM1	R*4	4-003454	001140	304	(152)
SEM2	R*4	4-004614	001140	304	(152)
SEQ	CHR	4-015060	001104	290	(58)
SQU	R*4	4-002314	001140	304	(152)
SUM	R*4	4-001154	001140	304	(152)
T	R*4	4-013720	001140	304	(152)
VAR	R*4	4-010260	001140	304	(152)

LABELS

Label	Address	Label	Address	Label	Address	Label	Address	Label	Add
10'	2-000000	20'	2-000004	25'	2-000010	30			
45	1-000520	50	**	60	**	65			
75	**	90	**	95	**	100'			

FUNCTIONS AND SUBROUTINES REFERENCED

CLOS$ OPEN$

T 1 Space Allocated = 021152 4405

```
      C ****** COMP ******
      C THIS PROGRAM FINDS THE CHI-SQUARED VALUE
      C RELATING THE DIFFERENCE BETWEEN TWO SIGNALS

0001          REAL CHI,NUM(152),DENOM(152),AVE1(152),AVE2(152)
0002          REAL T,VAR1(152),VAR2(152),M1,M2
0003          INTEGER N1,N2,S1,S2,STA,STO,N
0004          CHARACTER*10 FILE1,FILE2

      C READ IN FILES TO BE COMPARED

0005          TYPE*, ' ENTER FILE 1'
0006          READ(5,10), FILE1
0007          TYPE*, ' ENTER THE NUMBER OF FILES AVERAGED'
0008          TYPE*, ' INTO FILE 1'
0009          READ(5,20), N1
0010          TYPE*, ' ENTER FILE 2'
0011          READ(5,10), FILE2
0012          TYPE*, ' ENTER THE NUMBER OF FILES AVERAGED'
0013          TYPE*, ' INTO FILE 2'
0014          READ(5,20), N2
0015          TYPE*, ' ENTER THE STARTING SECOND FOR COMPARISON'
0016          READ(5,20), S1
0017          TYPE*, ' ENTER THE ENDING SECOND FOR COMPARISON'
0018          READ(5,20), S2

      10      FORMAT(A10)
0020  20      FORMAT(I2)
0021  40      FORMAT(F6.2,F6.1,F8.1)
0022          OPEN(UNIT=2,NAME=FILE1,FORM='FORMATTED',STATUS='OLD')
0023          OPEN(UNIT=3,NAME=FILE2,FORM='FORMATTED',STATUS='OLD')

      C READ IN THE MEAN AND VARIANCE FOR EACH POINT IN TIME
      C FROM EACH FILE

0024          DO 30 J=1,152
0025               READ(2,40), T,AVE1(J),VAR1(J)
0026               READ(3,40), T,AVE2(J),VAR2(J)
0027  30      CONTINUE
0028          CLOSE(2)
0029          CLOSE(3)
0030          M1=N1
0031          M2=N2

      C CALCULATE THE CHI-SQUARED VALUE

0032          DO 50 J=2,152
0033          NUM(J)=(AVE1(J)-AVE2(J))**2.0
0034          DENOM(J)=(((N1-1)*VAR1(J)+(N2-1)*VAR2(J))/(N1+N2-2))*(1/M1+1/M2)
0035  50      CONTINUE
0036          STA=S1*4
      7       STO=S2*4
      8       N=(STO-STA)
0039          CHI=0
0040          DO 60 L=STA,STO
0041               CHI=CHI+(NUM(L)/DENOM(L))
```

```
0        60     CONTINUE
0 ..3           TYPE*, ' N=.... ',N
0044            TYPE*, ' THE CHI-SQUARED VALUE IS .... ',CHI
0045            END
```

P RAM SECTIONS

Number	Name	Size		Attributes
1	$CODE1	001446	403	RW,I,CON,LCL
2	$PDATA	000436	143	RW,D,CON,LCL
4	$VARS	007166	1851	RW,D,CON,LCL
5	$TEMPS	000010	4	RW,D,CON,LCL

VARIABLES

Name	Type	Address	Name	Type	Address	Name	Type	Address	Name
CHI	R*4	4-000000	FILE1	CHR	4-007136	FILE2	CHR	4-007150	J
M1	R*4	4-007110	M2	R*4	4-007114	N	I*2	4-007134	N1
STA	I*2	4-007130	STO	I*2	4-007132	S1	I*2	4-007124	S2

ARRAYS

Name	Type	Address	Size		Dimensions
AVE1	R*4	4-002304	001140	304	(152)
AVE2	R*4	4-003444	001140	304	(152)
OM	R*4	4-001144	001140	304	(152)
.	R*4	4-000004	001140	304	(152)
VAR1	R*4	4-004610	001140	304	(152)
VAR2	R*4	4-005750	001140	304	(152)

LABELS

Label	Address	Label	Address	Label	Address	Label	Address	Label	Add
10'	2-000000	20'	2-000004	30	**	40'			
60	**								

FUNCTIONS AND SUBROUTINES REFERENCED

CLOS$ OPEN$

Total Space Allocated = 011302 2401

REFERENCES

Wilson, W.J., and Jones, G.M., (1979). Mammalian Vestibular Physiology. Plenum Press, New York, New York.

Benson, A.J., and Bodin, M.A.(1966). Interactions of linear and angular accelerations on vestibular receptors in man. Aerospace Med. 37, 144-154

Steinhausen, W. (1931). Uber den Nachweis der Bewegung der Cupula in der intakten Bogen gangsampulle des Labyrinthes bei der naturlichen rotatorischen und calorischen Reizung. Pflugers Arch. Ges. Physiol. 232, 500-512

van Egmond, A.A.J., Groen, J.J., and Jongkees, L.B. (1949). The mechanics of the semicircular canals. J Physiol. 110, 1-17

Robinson, D.A. (1977). Vestibular and optokinetic symbiosis: An example of explaining by modelling. In Control of Gaze by Brainstem Interneurons (R. Baker and A. Berthoz, eds.), pp. 49-58. Amsterdam:Elsevier

Raphan, T., Cohen, B. (1985). Chapter 8 in Adaptive Mechanisms in Gaze Control, pp. 123-124. Amsterdam:Elsevier

Malcolm, R. (1973). Ph.D. Thesis at McGill University, Montreal, Canada.

Goldberg, J.M., and Fernandez, C. (1971). Physiology of peripheral neurons innervating semi-circular canals of the squirrel monkey. I. Resting discharge and response to instant angular accelerations. J. Neurophysiol. 34, 635-660

Young, L.R., and Oman, C.M. (19[illegible]). Model of vestibular adaptation to horizontal rotation. Aerospace Med. 40, 1076-1080.

Oman, C.M. (1985). M.I.T. 16.251J Quantitative Physiology: Sensory and Motor Systems cLass notes.

Snedecor, G.W., and Cochran, W.G. (1967). Statistical Methods. Sixth Edition. The Iowa State University Press, Ames, Iowa.